NeuroImage: Clinical 15 (2017) 247–263

Contents lists available at ScienceDirect

NeuroImage: Clinical

journal homepage: www.elsevier.com/locate/ynicl

Amyloid positron emission tomography in sporadic cerebral amyloid angiopathy: A systematic critical update

Karim Farid[a,1], Andreas Charidimou[b,1], Jean-Claude Baron[c,*]

[a] Department of Nuclear Medicine, Martinique University Hospital, Fort-de-France, Martinique
[b] Massachusetts General Hospital, Department of Neurology, Stroke Research Center, Harvard Medical School, Boston, MA, USA
[c] U894, Centre Hospitalier Sainte Anne, Sorbonne Paris Cité, Paris, France

ARTICLE INFO

Keywords:
PET
CAA
PiB
Florbetapir
Microbleeds
Small vessel disease

ABSTRACT

Sporadic cerebral amyloid angiopathy (CAA) is a very common small vessel disease of the brain, showing preferential and progressive amyloid-βdeposition in the wall of small arterioles and capillaries of the leptomeninges and cerebral cortex. CAA now encompasses not only a specific cerebrovascular pathological trait, but also different clinical syndromes - including spontaneous lobar intracerebral haemorrhage (ICH), dementia and 'amyloid spells' - an expanding spectrum of brain parenchymal MRI lesions and a set of diagnostic criteria – the Boston criteria, which have resulted in increasingly detecting CAA during life. Although currently available validated diagnostic criteria perform well in multiple lobar ICH, a formal diagnosis is currently lacking unless a brain biopsy is performed. This is partly because in practice CAA MRI biomarkers provide only indirect evidence for the disease. An accurate diagnosis of CAA in different clinical settings would have substantial impact for ICH risk stratification and antithrombotic drug use in elderly people, but also for sample homogeneity in drug trials. It has recently been demonstrated that vascular (in addition to parenchymal) amyloid-βdeposition can be detected and quantified in vivo by positron emission tomography (PET) amyloid tracers. This non-invasive approach has the potential to provide a molecular signature of CAA, and could in turn have major clinical impact. However, several issues around amyloid-PET in CAA remain unsettled and hence its diagnostic utility is limited. In this article we systematically review and critically appraise the published literature on amyloid-PET (PiB and other tracers) in sporadic CAA. We focus on two key areas: (a) the diagnostic utility of amyloid-PET in CAA and (b) the use of amyloid-PET as a window to understand pathophysiological mechanism of the disease. Key issues around amyloid-PET imaging in CAA, including relevant technical aspects are also covered in depth. A total of six small-scale studies have addressed (or reported data useful to address) the diagnostic utility of late-phase amyloid PET imaging in CAA, and one additional study dealt with early PiB images as a proxy of brain perfusion. Across these studies, amyloid PET imaging has definite diagnostic utility (currently tested only in probable CAA): it helps rule out CAA if negative, whether compared to healthy controls or to hypertensive deep ICH controls. If positive, however, differentiation from underlying incipient Alzheimer's disease (AD) can be challenging and so far, no approach (regional values, ratios, visual assessment) seems sufficient and specific enough, although early PiB data seem to hold promise. Based on the available evidence reviewed, we suggest a tentative diagnostic flow algorithm for amyloid-PET use in the clinical setting of suspected CAA, combining early- and late-phase PiB-PET images. We also identified ten mechanistic amyloid-PET studies providing early but promising proof-of-concept data on CAA pathophysiology and its various manifestations including key MRI lesions, cognitive impairment and large scale brain alterations. Key open questions that should be addressed in future studies of amyloid-PET imaging in CAA are identified and highlighted.

1. Introduction

Sporadic cerebral amyloid angiopathy (CAA) is a very common small vessel disease (SVD) of the brain, a key cause of spontaneous lobar intracerebral haemorrhage (ICH) and a potential contributor to age- and Alzheimer pathology-related cognitive decline (Boulouis et al.,

* Corresponding author at: Department of Neurology, Sainte-Anne Hospital, Inserm U894, Paris Descartes University, Paris, France.
E-mail address: jean-claude.baron@inserm.fr (J.-C. Baron).
[1] Equal contribution.

http://dx.doi.org/10.1016/j.nicl.2017.05.002
Received 17 February 2017; Received in revised form 2 May 2017; Accepted 4 May 2017
Available online 05 May 2017

2016; Charidimou et al., 2012a; Viswanathan and Greenberg, 2011). CAA has thus received increasing attention in the both the Alzheimer and the stroke community for a number of additional important clinical reasons. In Alzheimer's disease there is likely a close relationship between CAA and the risk of amyloid-related imaging abnormalities (ARIA), the main dose-limiting adverse event to immunization against amyloid. ARIA shares important features with the CAA-related inflammation syndrome. In stroke, the presence of lobar cerebral microbleeds, and even more of cortical superficial siderosis – both putative CAA markers – may be associated with increased risk of future haemorrhage, including spontaneous lobar ICH, anticoagulation-related ICH and post-thrombolysis ICH.

The neuropathological hallmark of CAA is vascular amyloid-β deposition in the wall of small arterioles and capillaries of the leptomeninges and cerebral cortex, with or without involving the adjacent parenchyma. White matter small vessels, long cortical penetrators and deep arterial perforators (i.e. in the basal ganglia and thalami) do not typically show amyloid deposition. CAA should be viewed as a chronic degenerative protein-elimination failure process (Carare et al., 2013), in which the medial layer of arterioles undergoes progressive loss of smooth muscle cells with parallel deposition of amyloid, causing both haemorrhagic and ischemic lesions (Attems et al., 2011). This is mostly composed of the more soluble, amyloid-β_{40} species, in contrast to Alzheimer's disease amyloid plaques, primarily composed of amyloid-β_{42} species (Charidimou et al., 2012a). The vessels affected by CAA can show secondary (so-called vasculopathic changes), including fibrinoid necrosis, wall thickening, microaneurysm formation, and perivascular blood-breakdown products deposition (Love et al., 2014). The severity and extent of histological changes in CAA is often patchy (Vinters, 1987), whereby foci of vessels severely affected by CAA may be adjacent to other vessel segments with mild or absent amyloid-β deposition (Attems et al., 2011; Vinters, 1987). The regional topographical distribution typically favours posterior lobar brain regions (especially the occipital lobes and the temporal-parietal regions). During the course of the disease, CAA pathology progresses to more anterior lobar areas (Reijmer et al., 2016b). The cerebellum may also be occasionally affected (Vinters, 1987).

Results from population-based autopsy studies suggest that CAA of any neuropathological degree occurs in about 20–40% in non-demented, and 50–60% in demented elderly populations (age range for both groups 70–90 years) (Keage et al., 2009). Moderate-to-severe CAA occurs in about 7–24% and 30–40% of non-demented and demented older groups respectively (Keage et al., 2009). In Alzheimer's disease brains, any degree of CAA is identified in a high proportion of cases (85–95%) when sought thoroughly, often involving, at times even preferentially, the capillaries (Jellinger, 2002; Kalaria and Ballard, 1999). Nevertheless, in most these older individuals, CAA is asymptomatic and a relatively small proportion is diagnosed during life with CAA-related clinical symptomatology. CAA is most often suspected in life by symptomatic lobar (i.e. cortical-subcortical) ICH, especially involving the occipital and posterior parieto-temporal lobes (Rosand et al., 2005). Multiple recurrent CAA-related ICH can then occur over months or years (at a recurrence rate around 10%/year) (Biffi et al., 2010), with progressive neurologic decline and high risk of death. CAA is also associated with characteristic markers of SVD on clinical MRI, including lobar cerebral microbleeds and cortical superficial siderosis on T2*-GRE/SWI MRI, white matter hyperintensities and cortical microinfarcts on T2-weighted/FLAIR sequences, and MRI-visible perivascular spaces in the centrum semiovale on T2-weighted imaging (Greenberg et al., 2014). The presence of multiple strictly lobar microbleeds are accepted as one of the hallmark biomarkers for CAA presence and are useful for CAA diagnosis within the Boston criteria (Knudsen et al., 2001; Linn et al., 2010) (Table 1).

In this setting, the original Boston criteria for “probable CAA-related ICH” requires the occurrence of two symptomatic lobar ICHs or one symptomatic lobar ICH and the presence of ≥ 1 strictly lobar cerebral microbleed in a patient ≥ 55 years old, other potential causes being excluded (Knudsen et al., 2001). “Probable CAA-related ICH” is the category pointing to the highest certainty for CAA diagnosis within the Boston criteria, with sensitivity ~90% and specificity ~80–85%. The addition of cortical superficial siderosis as another haemorrhagic marker was recently shown to improve the sensitivity of these criteria (i.e. revised Boston criteria) (Linn et al., 2010). Similar criteria have now been validated against CAA-proven histopathology even in individuals presenting without ICH in a hospital-based setting: specificity > 90% and positive predictive value > 87% in the presence of ≥ 2 strictly lobar CMBs, and no other cause identified (Martinez-Ramirez et al., 2015). This is of particular clinical relevance, as CAA is increasingly recognized to present without overt ICH, including transient focal neurological episodes (‘amyloid spells’) (Charidimou et al., 2013a; Charidimou et al., 2012b) often associated with acute convexity subarachnoid haemorrhage, focal seizures or cognitive impairment and dementia. CAA may also be an incidental diagnosis in patients with ischaemic stroke, in which it is considered an important risk factor for ICH related to oral anticoagulants and thrombolysis-related haematomas (Charidimou et al., 2015d; Mattila et al., 2015). However, CAA diagnosis in patients without ICH and low CMBs counts or patients with only a single lobar ICH (i.e. “possible CAA” as per Boston criteria) remains challenging and with relatively low specificity. In any case, a

Table 1
Boston criteria for the diagnosis of CAA. Classic criteria are based only on the presence of lobar CMBs and ICH (not cSS).

Definite CAA	Full post-mortem examination demonstrating: – Lobar, cortical or corticosubcortical haemorrhage/microbleed – Severe CAA with vasculopathy – Absence of other diagnostic lesion
Probable CAA with supporting pathology	Clinical data and pathologic tissue (evacuated hematoma or cortical biopsy) demonstrating – Lobar, cortical or corticosubcortical haemorrhage/microbleed – Some degree of CAA in specimen – Absence of other diagnostic lesion
Probable CAA	Clinical data and MRI or CT demonstrating – Multiple haemorrhages/microbleeds restricted to lobar, cortical or corticosubcortical regions (cerebellar haemorrhage allowed) OR – Single lobar, cortical or corticosubcortical haemorrhage/microbleed and focal or disseminated superficial siderosis[a] AND Age ≥ 55 years AND Absence of other cause of haemorrhage or superficial siderosis
Possible CAA	Clinical data and MRI or CT demonstrating – Single lobar, cortical or corticosubcortical haemorrhage/microbleed OR – Focal or disseminated superficial siderosis[a] AND Age ≥ 55 years AND Absence of other cause of haemorrhage or superficial siderosis

[a] The revised Boston criteria incorporate cSS in patients presenting with lobar ICH.

definite diagnosis still rests on autopsy as the gold standard, while biopsy samples of adequate quality can provide further support for CAA diagnosis ('probable CAA with supportive pathology') (Knudsen et al., 2001).

While the clinical-imaging spectrum of CAA has been expanded and refined substantially with the broad availability of brain MR imaging (Boulouis et al., 2016), imaging biomarkers of brain parenchymal microvascular lesions provide only indirect evidence for the disease. Since symptomatic or asymptomatic CAA presentations with or without ICH are becoming increasingly common clinical scenaria, additional non-invasive techniques and more direct biomarkers to diagnose CAA in vivo would have major clinical impact. Such a biomarker would be particularly useful for detecting CAA pathology in patients where the diagnosis is currently uncertain. Examples would include single lobar ICH without microbleeds (possible CAA), mixed location of haemorrhagic lesions (ICH and/or CMBs in both lobar and deep areas, the latter being associated with chronic arterial hypertension and other vascular risk factors), as well as strictly lobar microbleeds or cortical superficial siderosis in people with a history of ischemic stroke, isolated cognitive impairment or subacute encephalopathy, or even asymptomatic (e.g., patients with atrial fibrillation considered for anticoagulation). Of note, even in the setting of probable CAA-ICH by the Boston criteria, these is still an element of uncertainty, especially in 'borderline' cases with one lobar ICH and only one or two lobar microbleeds. Also, the Boston criteria require 'all other ICH causes to be excluded' (Table 1), which is often not straightforward in clinical practice, since many factors could potentially contribute to a symptomatic ICH or to lobar microbleeds, on top of lowering the threshold for CAA expression. Along this line, in the elderly brain hypertensive arteriopathy often co-exists with CAA and can also lead to (or strongly facilitate) lobar ICH and CMBs. A molecular diagnosis would be very useful across different patient populations. This would have substantial individual clinical impact in risk stratification for anticoagulants or antithrombotic drug administration in elderly people with vascular risk factors, ischaemic events, atrial fibrillation, or spontaneous ICH and small vessel disease in general, but also for appropriate selection of patients for drug trials and other clinical studies and for monitoring of drug effects.

Vascular amyloid-β can be detected and quantified on positron emission tomography (PET) scanning with the amyloid radioligand tracer ^{11}C-labelled Pittsburgh Compound B (PiB), and might thus serve as a direct, molecular marker of underlying CAA. Although PiB was initially developed to label parenchymal amyloid-β deposits in Alzheimer's disease, it also labels cerebrovascular amyloid (Bacskai et al., 2002). A radiologic-pathologic study showed high cortical PiB-PET retention in a patient diagnosed with Lewy body dementia, in whom post-mortem amyloid immunohistochemistry three months later revealed only moderate parenchymal amyloid plaque number, but abundant vascular amyloid deposition (Bacskai et al., 2007). A number of small early studies have reported positive PiB-PET in non-demented patients with pathology-proven sporadic or mutation-proven familial CAA (Greenberg et al., 2008; Johnson et al., 2007). This raised the potentially exciting prospect of making a CAA diagnosis in living subjects with high sensitivity and specificity using amyloid imaging and without the need for a brain biopsy in the appropriate clinical setting. However, healthy controls also frequently show abnormally high PiB uptake thought to reflect incipient Alzheimer pathology (Mintun et al., 2006; Rowe et al., 2013), pointing to potentially limited diagnostic utility of amyloid PET in CAA due to poor specificity, while the differentiation between CAA- and AD-related abnormally high PiB uptake is another potential source of reduced specificity (Baron et al., 2014). Apart from its diagnostic potential, amyloid PET imaging is increasingly used in CAA research to directly test pathophysiological/mechanistic hypotheses on CAA-related brain lesions, including haemorrhagic markers (Dierksen et al., 2010; Gurol et al., 2012) and the underlying presumed pathology, i.e. cerebrovascular amyloid.

In this article, we aim to systematically review and critically appraise the published literature on amyloid-PET (PiB and other tracers) in CAA, using standard 'late phase' imaging, but also the recently highlighted 'early phase' imaging. We focus on two key areas: (a) the diagnostic utility of amyloid-PET in CAA, including a practical algorithm based on the available evidence; and (b) the use of amyloid-PET as a window to understand pathophysiological mechanisms of the disease. Of note, all the PET studies in CAA published to date have used amyloid PET tracers, i.e., no article on CAA using other PET tracers such as FDG have appeared thus far. Where relevant, limitations and gaps in the literature are highlighted, with recommendations for future studies. Finally, our paper focusses on the more common and clinically relevant at a larger scale sporadic CAA, rather than the rare hereditary CAA syndromes (Greenberg et al., 2008) and hereditary systemic transthyretin amyloidosis with CAA (Sekijima et al., 2016) for which PET studies remain extremely limited.

2. Methods: search strategy and literature review

We searched PubMed from inception until September 1, 2016 using a combination of keyword search and MeSH terms: (PET OR PiB OR Pittsburgh OR positron emission tomography) AND (amyloid angiopathy). Reference lists from all included articles, review papers on the topic and the authors' own files were also searched for relevant studies in English. Two authors identified potentially relevant studies: (a) on the diagnostic utility of amyloid PET in sporadic CAA (excluding case reports and studies only including AD patients); (b) on potential pathophysiological mechanism of brain injury in sporadic CAA; and (c) other relevant studies on CAA. The final list of references was decided upon consensus between all co-authors, based on their relevance to the themes covered in this review.

2.1. Data extraction

Two authors independently extracted data from all eligible studies on comparison groups i.e., CAA, healthy controls (HC), AD, CAA clinical presentation, imaging analysis method and main results. For the CAA and HC groups, relevant data on PiB-PET amyloid positivity were extracted if available, or calculated, and sensitivity and specificity were derived from these data.

3. Results

Based on our search criteria, we identified 94 publications, of which we retained 17 for the present study. Fig. 1 presents the flow chart for exclusion of studies.

3.1. Diagnostic utility of amyloid PET in sporadic CAA (Table 1)

3.1.1. Late amyloid brain uptake

3.1.1.1. CAA vs healthy controls (HCs). Four papers have provided data comparing late amyloid uptake in CAA and HCs (Baron et al., 2014; Gurol et al., 2012; Johnson et al., 2007; Ly et al., 2010a), although in one study this was not the primary aim (Gurol et al., 2012). Of note, HCs recruited into these studies had no cognitive complaint and had normal MMS; only Gurol et al., 2013 did not report specifically on the cognitive status of their HCs. Table 2 provides a summary. In total, the data from 71 patients were reported (67 diagnosed as probable CAA, 4 as possible CAA), and of 87 age-matched HCs. Interestingly, Baron et al. used 3T T2*-GRE MRI to assess the presence of microbleeds in the HCs and excluded post-hoc one HC based on the presence of > 2 lobar microbleeds, i.e., potentially due to asymptomatic CAA. Among reported CAA patients, there were 48 lobar ICH cases and 27 with non-ICH presentations (mainly seizures, cognitive complaints, subacute encephalopathy). Two studies reported only CAA-lobar ICH patients (Baron et al., 2014; Ly et al., 2010a), and the remaining two mixed-presentations CAA samples.

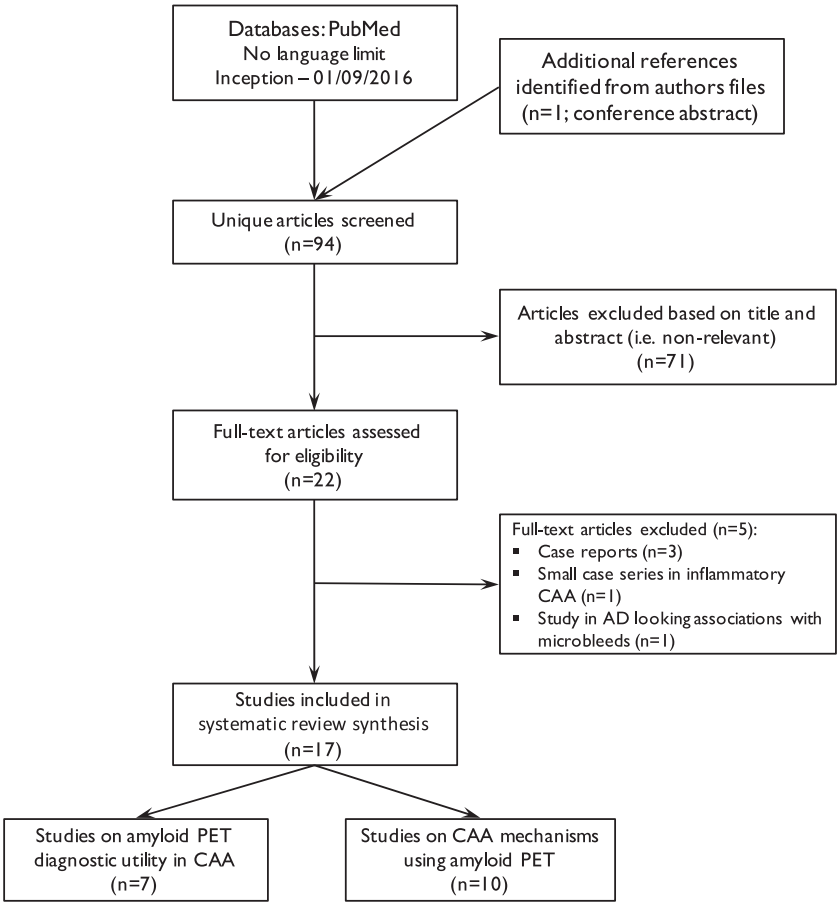

Fig. 1. Flow chart of study identification and selection.

All four studies used PiB and fully quantitative analysis by kinetic modelling of the whole time-activity curves to derive the distribution volume ratio (DVR, using the cerebellum as reference tissue) as an index of specific binding, using the values averaged across the whole cortex. Three of them also used regional analysis and cortical regions of interest (ROI) ratios (Johnson et al., 2007), Ly et al., 2010a, 2010b, Baron et al., 2014). Of note, the brain regions affected by previous haemorrhages were consistently excluded from the analysis. Two studies also used simple visual analysis of the brain uptake images obtained in the late period after tracer injection (normalized to injected dose and subject's weight, so-called standardized uptake values or SUV, and divided by mean cerebellar SUV, generating SUVr images), (Baron et al., 2014).

Using DVR, three studies reported significantly higher cortical PiB uptake in CAA patients in comparison with HCs (Gurol et al., 2012; Johnson et al., 2007; Ly et al., 2010a), while one study found no significant difference (Baron et al., 2014).

Individual analysis comparing PiB positivity in CAA patients vs controls was reported in three studies (Baron et al., 2014; Johnson et al., 2007; Ly et al., 2010a). The reference diagnostic standard in all analyses was CAA according to the Boston criteria (Table 1). Using visual analysis, Johnson et al. (Johnson et al., 2007) found positive PIB PET in all probable CAA patients, as well as in 6/15 aged-matched HCs. Using the 75% percentile of the aged-matched HC group as cut-off, Ly et al. (2010a) reported PiB positivity in 9/12 CAA patients (7/8 probable CAA and 2/4 possible CAA); by definition, 25% of the aged-matched HCs were therefore PiB +. Using as DVR cut-off the 95% upper confidence limit from 10 young (< 55 years) HCs as control group to account for the frequent positivity known to be present in older HCs, Baron et al. (Baron et al., 2014) found 10/11 positive PIB in probable CAA patients, and in 4/9 aged-matched HCs. Using visual analysis, the values were 9/11 and 4/9, respectively, indicating lower sensitivity than with the quantitative method.

Only one study (Baron et al., 2014) formally reported on sensitivity and specificity of PiB-PET for CAA diagnosis. Based on the above data, they reported a sensitivity of 91%, a specificity of 55%, a positive predictive value of 71%, and a negative predictive value of 83%. As will be addressed in the Discussion section, similar data can however be calculated from two other studies based on reported raw data (Johnson et al., 2007; Ly et al., 2010a).

Similarly, only one study (Baron et al., 2014) compared the regional PiB uptake data (corrected for grey matter atrophy) between probable CAA and aged-matched HCs, reporting no significant difference for any regional cortical DVR value between the two groups. Based on the neuropathological evidence of more severe CAA pathology in the posterior, and particularly occipital, cortical areas, this study also assessed the occipital/whole cortex and frontal/whole cortex ratios, and again found no significant difference between the two comparison groups.

3.1.1.2. Comparison between probable CAA-ICH and deep ICH. Two studies used deep (presumably hypertensive, non-CAA) ICH as controls to assess amyloid PET in lobar (presumably CAA-related) ICH (Gurol et al., 2016; Raposo et al., 2014a, 2014b). See Table 1 for details. Of note, the Raposo et al. (2014a, 2014b) study has been published as an abstract only, and many important clinical details are missing. In total, 28 lobar and 30 deep hypertension-related ICHs were studied (Raposo et al., 2014a, 2014b). Of the lobar ICHs, Gurol et al. (2016) and Raposo et al. (2014a, 2014b) studied 10 patients with probable CAA each, and the latter authors also studied 4 patients with possible CAA (note: 4 lobar ICH patients categorized as neither probable nor possible CAA based on their abstract). Both studies used

Table 2
Summary of studies focusing on the diagnostic utility of amyloid PET imaging in CAA.

Study	Comparison groups (*n*, age (yrs ± SD)	CAA presentation	Image analysis	Main results	Comments
Late phase amyloid imaging					
(Johnson et al., 2007)[a]	1) Probable CAA (*n* = 6, 68.5 ± 11.4) 2) HC (*n* = 15, 72.7 ± 6.4); MMSE: 29.1 ± 0.9 3) Probable spAD (*n* = 9, 71.4 ± 10.9)	Seizure (*n* = 4); LICH (*n* = 2)	Three methods: ✓ Visual; ✓ DVR (cerebellum) ✓ SUVR (pons)	✓ Visual: CAA: 6/6 + ve: AD: 9/9 + ve; HC: 6/15 + ve ✓ Whole cortex DVR & SUVR: AD > CAA > HC, $p < 0.001$ ✓ Occ/global DVR & SUVR: CAA > AD, $p < 0.01$	✓ CAA patients: non demented ✓ Brain regions with structural damage removed from the analysis ✓ Same results with DVR and SUVR ✓ No individual quantitative analysis; no cutoff reported
(Ly et al., 2010a)[a]	1) CAA (*n* = 12, 73.9 ± 10.3); (possible *n* = 4) (probable *n* = 8) 2) AD: (*n* = 13, 73.8 ± 11.7) 3) HC: (*n* = 22, 71.8 ± 6.6)	LICH	DVR (cerebellum)	✓ CAA 9/12 (75%) + ve (probable CAA = 7; possible CAA = 2) ✓ Neocortical DVR: ✓ AD > CAA > HC, $p < 0.01$ ✓ Occ/neocortical: CAA > AD; $p < 0.01$ ✓ Frontal/neocortical: AD > CAA; $p < 0.05$	✓ CAA (*n* = 2) with mild cognitive decline ✓ Brain regions with structural damage removed from the analysis ✓ Neocortical DVR cut-off: 75% percentile of the age-matched HCs
(Gurol et al., 2013)[a]	1) Probable CAA (*n* = 42, 68 ± 10) 2) AD (*n* = 43, 74 ± 7.4); (AD *n* = 18) MCI *n* = 25) 3) HC (*n* = 50, 73.3 ± 7)	LICH (*n* = 23); other (*n* = 19)	DVR (cerebellum)	Whole cortex DVR: AD = CAA > HC; $p < 0.001$	✓ CAA patients: non demented ✓ No individual quantitative analysis of CAA patients
(Baron et al., 2014)[a]	1) Probable CAA (*n* = 11, 70 ± 7) 2) HC (*n* = 9, 65 ± 5)	LICH	Two methods: ✓ Visual; ✓ DVR (cerebellum)	✓ Visual: CAA 9/11 + ve; HC 4/9 + ve ✓ Whole cortex DVR: 10/11 + ve CAA; 4/9 + ve HC ✓ Whole cortex and regional DVR: CAA vs HCs; p = NS ✓ Occ/whole cortex: CAA < HC; p = NS ✓ Frontal/whole cortex: HC > CAA, p = NS	✓ CAA patients: non demented brain regions ✓ Brain regions with structural damage removed from the analysis ✓ Whole cortex DVR cut off: 1.22 (95% upper limit from *n* = 10 HC < 55 yrs. old) ✓ Single CAA patients with negative whole cortex DVR: value just below the cutoff ✓ Calcarine/frontal DVR ratio: CAA > AD (*n* = 7); $p < 0.05$
(Gurol et al., 2016)[b]	1) Probable CAA (*n* = 10, 66.9 ± 7) 2) 2) HTN-related deep ICH (*n* = 9, 67.1 ± 8)	LICH	Three methods: ✓ Visual; ✓ SUVR (cerebellum) ✓ DVR (cerebellum)	✓ Visual: CAA 10/10 + ve, HTN-ICH 1/9 + ve ✓ Whole cortex SUVR: CAA > HTN-ICH, $p = 0.001$ ✓ Occ/global: CAA > HTN-ICH, $p < 0.03$; other lobes: NS	✓ Brain regions with structural damage removed from the analysis ✓ Whole cortex SUVR values showed no overlap between the visually-determined amyloid positive and negative groups; retrospectively determined cut-off: 1.21
(Raposo et al., 2014a, 2014b)[b]	1) CAA (*n* = 18), probable CAA (*n* = 10), possible CAA (*n* = 4) 2) Deep ICH (*n* = 21)	LICH	SUVR (cerebellum)	✓ Whole cortex SUVR: CAA > deep ICH; $p = 0.01$ probable CAA > possible CAA; $p < 0.05$	✓ Reported in abstract form only ✓ 4 pts. with lobar ICH neither probable not possible CAA; cause not reported ✓ Deep ICH: cause not reported
Early phase amyloid imaging					
(Farid et al., 2015)[a]	1) Probable CAA (*n* = 11, 70 ± 7) 2) HC (*n* = 9, 65 ± 5) 3) 3) AD (*n* = 7, 66 ± 5)	LICH	SUVR (cerebellar vermis)	■ Whole cortex SUVR: CAA 6/11 + ve, HC 0/9 + ve; CAA < HC, $p < 0.05$ ■ Occ/PCC SUVR ratio: CAA < HC, p = NS CAA < AD, $p < 0.002$ AD > HC, $p = 0.001$	■ Same CAA and HC population as Baron et al. (2014) ■ Brain regions with structural damage removed from analysis ■ Whole cortex SUVR cut off: 0.94 (95% upper limit from *n* = 10 HC < 55 yrs. old) ■ No cut-off or individual analysis reported for the occ/PCC ratio.

CAA: cerebral amyloid angiopathy; HC: healthy control; spAD = sporadic Alzheimer disease; ICH: intracerebral haemorrhage; L: lobar; HTN: arterial hypertension; SUVR: standard uptake value ratio (reference structure); DVR: distribution volume ratio (reference structure); + ve: positive amyloid scan; Occ: occipital cortex; PCC: posterior cingulate cortex.

[a] PiB.

[b] Florbetapir.

^{18}F-flobetapir, and both performed whole cortex SUVR analysis using the cerebellum as reference. In addition, Gurol et al. performed regional SUVR and DVR analyses, as well as visual analysis.

Both studies report significantly higher whole cortex SUVR in lobar vs deep ICH. Also, Raposo et al. (2014a, 2014b) found significantly higher amyloid burden in probable as compared to possible CAA lobar ICH. Based on visual analysis, Gurol et al. (2016) found positive amyloid PET in all 10 probable CAA patients, vs 1/9 deep ICH, i.e. a sensitivity of 100% and a specificity of 89%. Raposo et al. (2014a, 2014b) did not report on individual visual classification. Only Gurol et al. (2016) reported on regional ^{18}F-flobetapir uptake. These authors found a significantly higher occipital/global uptake ratio in probable CAA-related as compared to hypertension-related deep ICH.

3.1.1.3. Comparison between probable CAA and Alzheimer's disease (AD). As will be extensively addressed in the Discussion section, given the relatively high occurrence of amyloid PET positivity with AD pattern in aged controls, one major issue regarding the diagnostic utility of this approach in suspected CAA patients is whether a significant difference exists in the regional distribution pattern of abnormal amyloid deposition as detected in vivo by PET (Baron et al., 2014). To (overtly or covertly) address this issue, three articles, all using PiB, have compared amyloid uptake in probable CAA vs probable AD patients (Gurol et al., 2012; Johnson et al., 2007; Ly et al., 2010a) (Table 2).

Two studies (Johnson et al., 2007; Ly et al., 2010a) found a significantly higher whole cortex PiB uptake (either DVR ort SUVR) in AD than in CAA, while Gurol et al. (2013) reported no significant difference. Based on the notion that CAA is more severe in occipital regions (Kovari et al., 2013; Vinters, 1987; Vinters and Gilbert, 1983), which conversely are largely spared in AD, both groups compared the occipital/whole cortex or neocortex uptake between the two patient populations, predicting a higher ratio in CAA. Effectively, both groups found a significantly higher occipital/whole cortex PIB ratio in CAA than in AD patients for either DVR or SUVR. As a corollary, the frontal/neocortical PiB uptake ratio was significantly higher in AD than in CAA patients in the Ly et al. (2010a).

Only Johnson et al. (2007) assessed the diagnostic value of PiB PET in CAA vs AD. Using visual analysis, they found PiB positivity in 100% of patients of either group. No study has reported on the diagnostic value of regional uptake for differentiating CAA from AD, either using quantitative ratios or visually.

As will be seen in the Discussion section, one study (Baron et al., 2014) mentioned findings regarding the comparison of CAA vs AD as ancillary data in their study comparing probable CAA patients to healthy controls.

For illustration purposes, Fig. 2 presents typical PiB uptake images in aged healthy controls, CAA and AD.

3.1.2. Early PiB uptake

One recent study reported on the use of early PiB uptake in CAA (Farid et al., 2015). The underlying idea was based on the well-established notion that early tracer entry in brain tissue reliably reflects perfusion, which in turn could have diagnostic value in the study of CAA. Importantly, in the resting state brain perfusion is highly correlated with FDG uptake, and effectively several studies have shown that early PiB or ^{18}F-flobetapir uptake is indeed well correlated with FDG uptake in healthy controls and AD, and can be used as a proxy of brain energy metabolism (Forsberg et al., 2012; Rostomian et al., 2011; Rodriguez-Vieitez et al., 2017). Thus, using both the early and late tissue uptake of amyloid tracers could, from the same PET session, provide information on both neurodegeneration/parenchymal and cerebrovascular amyloid burden.

3.1.2.1. Probable CAA vs aged-matched healthy controls. Farid et al. (2015) used the PET data from the 1–6 min frame after PiB administration and generated atrophy-corrected SUVR images using the cerebellar vermis as reference tissue, and compared 11 non-demented patients with probable CAA-related lobar ICH to 9 aged-matched HCs with normal MMSE (same population as in (Baron et al., 2014)). Using regional quantitative analysis (excluding the areas of previous haemorrhage), CAA patients had significantly lower early-phase PiB whole cortex uptake than HCs. Using as cut-off the 95% lower confidence limit from 10 young controls as detailed above (Baron et al., 2014), none of the HCs had whole cortex early PiB uptake below this cut-off whereas 6/11 CAA patients did. Thus, the sensitivity was 55%, the specificity 100%, the predictive positive value was 100% and the predictive negative value was 64% for CAA diagnosis using early PiB-PET data.

3.1.2.2. Probable CAA vs AD. The same authors (Farid et al., 2015) compared regional early PiB uptakes between probable CAA and AD. Based on known pathological distribution of lesions in CAA (see above) and pretesting state perfusion/FDG uptake in AD, they focused on the occipital and posterior cingulate cortices. Consistent with these notions, they found significantly lower occipital early PiB uptake in CAA than AD, but no significant difference regarding the posterior cingulate area. Consequently, the occipital/posterior cingulate ratio was significantly lower in CAA than in AD (Fig. 3). Sensitivity and specificity for this ratio is not presented given the small AD sample used (n = 7).

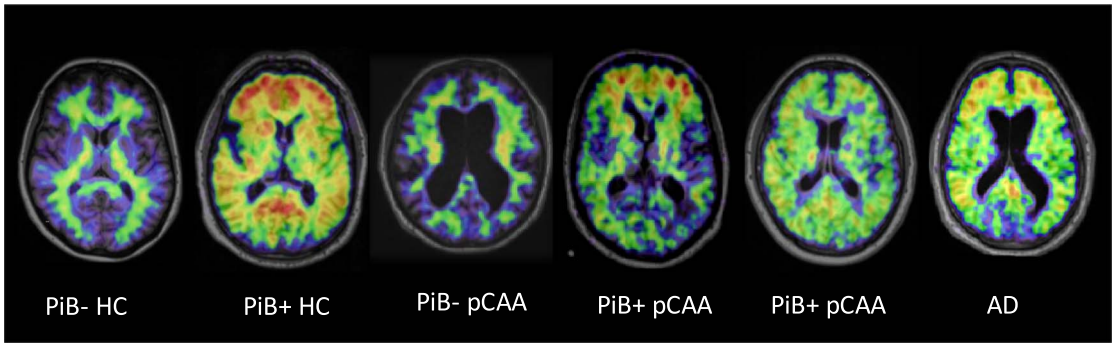

Fig. 2. Typical PiB uptake images (one axial brain cut) in aged healthy controls (HC), probable CAA and AD. From left to right are shown examples of i) normal scan (i.e., PiB −) in an aged HC; ii) positive PiB scan (i.e., PiB +) in another aged HC, adopting the typical 'Alzheimer disease (AD)-like pattern', namely uptake highest in frontal cortex; iii) PiB-probable cerebral amyloid angiopathy (pCAA) subject; iv) PiB + pCAA subject, AD-like pattern; v) PiB + pCAA subject, with 'CAA-like pattern', namely equal uptake in occipital and frontal cortex; and vi) PiB + AD subject, AD-like pattern. Note that these images are shown only for illustrative purposes as significant overlap exists between these typical patterns across clinical entities (see Discussion).

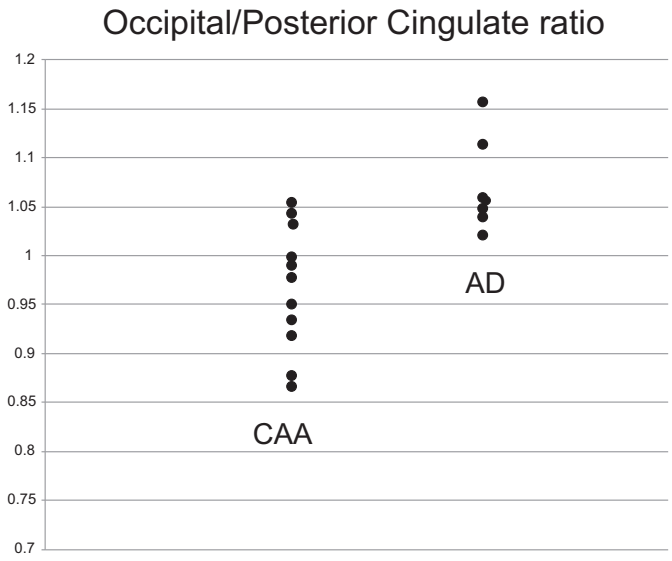

Fig. 3. Early-phase PiB Occipital/Posterior cingulate cortex uptake ratio in probable CAA and AD. The difference in ratio between the two groups is highly significant ($p = 0.002$; Mann-Whiney test). This graph shows the presence of a substantial though limited overlap between the two populations, with a ratio around one discriminating all AD subjects vs 9/11 CAA subjects. See Methods and (Farid et al., 2015) for details.

3.2. PET as a window to explore pathophysiological mechanisms in CAA (Table 3)

3.2.1. Haemorrhagic manifestations

In a cross-sectional study of 16 patients with probable CAA, significantly higher PiB DVR was detected at sites of lobar microbleeds as compared to other locations, suggesting that high local vascular amyloid burden probably underlies vascular rupture causing microbleeds (Dierksen et al., 2010). In a longitudinal study of 11 patients with probable CAA, PiB retention at baseline was higher at regions-of-interest (ROIs) that developed new lobar CMBs or ICH at > 1-year follow-up MRI, providing further evidence that vascular amyloid burden contributes to the occurrence of new lobar CMBs and ICHs (Gurol et al., 2012). In a completely different perspective, another study (Ly et al., 2010b) reported higher PiB binding in patients with vs those without post-thrombolysis parenchymal haemorrhage, but not for differentiating simple haemorrhagic transformation, suggesting a role for vascular amyloid burden in t-PA-related brain haemorrhage susceptibility. The location of the parenchymal hematoma, i.e. within or remote from the ischemic area, was not detailed.

Ly et al. (2015) reported a case series of seven patients with non-aneurysmal convexity subarachnoid haemorrhage (cSAH) fulfilling the Boston criteria for probable CAA who all showed a positive PiB scan by visual analysis, reinforcing the idea of a relationship between vascular amyloid burden and cSAH. Dhollander et al. (2011) and Na et al. (2015) investigated the relationship between PiB uptake and cortical superficial siderosis (cSS). The former reported a significantly higher PiB uptake in the immediate vicinity of cSS in two probable CAA patients, while the latter found a close relationship between the presence of cSS and PiB positivity in a large sample of patients with AD or subcortical vascular cognitive impairment (SVCI), such that PiB was positive in 100% of the patients with cSS ($n = 12$) as compared to 57% of the subjects without cSS. In other words, cSS was never present in PiB-patients, supporting the idea that a vascular amyloid process underlies cSS. Although application of the Boston criteria in the patients of this study is not presented, it can be assumed that cSS was part of the spectrum of CAA either in isolation or in association with AD pathology.

3.2.2. White matter changes

So far, only one study has addressed the relationship between hemispheric white matter hyperintensities (also called leukoaraiosis) and amyloid binding in probable CAA (Gurol et al., 2013). To test the specificity of the association, these investigators also included non-CAA cohorts where WMHs are also frequently encountered, namely aged healthy controls and AD patients. This study found a strong correlation between leukoaraiosis volume and global PiB DVR in probable CAA patients, which was not present in healthy controls or AD, suggesting that it is the vascular, not the parenchymal amyloid, that drives this association. In other words, vascular amyloid affecting the penetrating cortical arterioles might directly cause chronic white matter ischemia and hence leukoaraiosis.

A more recent study (Charidimou et al., 2015a) investigated the relationship between enlarged perivascular spaces (PVS) in the centrum-semi-ovale (CSO), a recently proposed new potential MR marker of CAA, and PiB burden. They found a significant relationship between the number of CSO-PVS and whole cortex PiB DVR across both probable CAA patients and elderly healthy controls, as well as within each group separately. Importantly, no such relationship was observed for basal ganglia PVS, which have been more closely associated with hypertensive arteriopathy. These findings suggested that amyloid burden in the penetrating cortical arterioles in some way might cause or contribute to CSO-PVS across the aging and CAA spectrum (Charidimou et al., 2015a).

3.2.3. Cognitive manifestations

In CAA, vascular amyloid leads to various types of brain damage, including focal and more widespread parenchymal brain injury. Accordingly, slowly progressive cognitive manifestations are frequently associated with CAA. One subtype of cognitive presentation of CAA is however subacute, in the form of an encephalopathy or rapidly progressing dementia related to CAA-induced inflammation with marked focal hemispheric white matter vasogenic edema and rapid response to corticosteroids (Carmona-Iragui et al., 2016). Although the finding of multiple lobar microbleeds is now part of the diagnostic criteria (Linn et al., 2010), some patients still go on to have a brain biopsy, with attending risks. A small case series study (Carmona-Iragui et al., 2016) reported 4 patients with cognitive manifestations due to CAA-related inflammation, two of which had a PiB scan over a year after their episode. Both patients were PiB positive by visual assessment, suggesting a potential usefulness of amyloid PET in the work-up of these patients.

Using MR-based diffusion tensor imaging (DTI) a single center study (Reijmer et al., 2015) assessed global network efficiency in a large sample of probable CAA patients. As compared to aged healthy controls, global network efficiency was significantly reduced in CAA patients and was related to MR-markers of CAA. In the subsample of CAA patients who underwent a PiB scan, global network efficiency was related to higher cortical PiB DVR, including an association with the regional distribution of the two measures, i.e., more posterior amyloid burden related to more posterior network disruption, suggesting that network efficiency partly mediates the relationship between vascular amyloid burden and cognitive impairment.

4. Discussion

4.1. Diagnostic value

The ultimate aim of in vivo non-invasive diagnostic tests in CAA is to replace the need of brain biopsy/autopsy to make a definite formal diagnosis of CAA. This would have clinical impact in ‘probable CAA’ according to the Boston criteria, which has very good but imperfect diagnostic accuracy, but especially for the ‘possible CAA’ category, as detailed in the Introduction.

4.1.1. Summary of main findings: whole-cortex tracer uptake

Six publications have addressed (or reported data useful to address)

Table 3
Summary of main studies providing mechanistic insights using amyloid PET imaging in CAA.

Study	Topic	Patient population [*n*; age (yrs ± SD)]	Clinical presentation	Image analysis	Main results	Comments
(Dierksen et al., 2010)[a]	Microbleeds	Probable CAA (n = 16; 64.0 ± 11.8)	LICH (n = 9)	DVR (cerebellum)	Significant relationship between PiB retention and microbleeds location	7 pathology-confirmed CAA patients
(Ly et al., 2010a)[a]	Post-thrombolysis ICH	HC (n = 15; 74) ICH (n = 7; 77) No ICH (n = 8; 77)	Ischemic stroke treated with rt.-PA within 3 h	DVR (cerebellum)	Higher PiB binding in patients with vs those without ICH and vs HCs	No symptomatic ICH studied. Topography of ICH (within or remote from infarct) not assessed. PiB not increased in simple haemorrhagic transformation.
(Gurol et al., 2012)	Prediction of new ICH	Probable CAA (n = 11; 70.9 ± 8.6)	LICH (n = 5) Other (e.g., seizure, gait problems; n = 6)	DVR (cerebellum)	New CAA-related haemorrhages (CMBs or ICH) occur preferentially at sites of increased amyloid deposition	PiB uptake in a superior frontal/parasagittal aggregate ROI was predictive of the number of new haemorrhages.
(Dhollander et al., 2011)[a]	cSS	Probable CAA (n = 1; 76); possible CAA (n = 1; 72)	cSS	DVR	PiB uptake significantly higher in the immediate vicinity of cSS	–
(Na et al., 2015)[a]	cSS	Whole sample (n = 232; 72.2 ± 8.1) 1) AD (n = 90) 2) SVCI (n = 142)	cSS (n = 12) No cSS (n = 220)	SUVr	cSS present in both AD and SVCI, but never in PiB (−) patients, supporting the hypothesis that cSS reflects an amyloid rather than ischemic process	− SVCI patients with cSS very likely to be PiB + − PiB + pattern in cSS not typical for CAA
(Ly et al., 2015)[a]	cSAH	Probable CAA, n = 7 (n = 2 with supporting pathology)	Non-aneurysmal cSAH	Visual analysis of summed 40-70 min images	7/7 PiB + 'consistent with CAA'	Case series of 7 patients; no comparison to healthy controls or AD patients. PiB PET performed 3–36 months after cSAH. Three pts. had LICH at follow-up: no clear topographical relationship with PiB cortical burden.
(Gurol et al., 2013)[a]	WMH	1) Probable CAA (n = 42, 68 ± 10) 2) AD (n = 43, 74 ± 7.4) 3) 3) HC (n = 50, 73.3 ± 7)	LICH (n = 23) Other (n = 19)	DVR (cerebellum)	Global PiB retention and WMH showed strong correlation (rho = 0.52, p < 0.001) in the CAA group but not in HC or AD	No significant PiB-WMH correlation in AD and HCs.
(Charidimou et al., 2015a)[a]	CSO-PVS	1) Probable CAA (n = 11; 71) 1) 2) HC (n = 20; 59.5); (age < 60, n = 10; age > 60, n = 10)	LICH	DVR	PIB retention higher in high vs low CSO-PVS degree (p = 0.0007).	Whole cortex PiB retention associated with CSO-PVS degree both as continuous (p = 0.040) and dichotomous variable p = 0.002). Finding present both in the whole sample (HC + CAA) and in CAA only. No significant relationship between PiB and basal ganglia PVS.
(Carmona-Iragui et al., 2016)[b]	CAA-ri	Probable CAA-ri (n = 4); two patients only underwent PET	CAA-ri	SUVr (visual assessment)	Both patients PiB +	PET performed 13–19 months after corticosteroids. Pre-treatment PET not obtained. No comparison to HCs or AD. Lower PiB uptake in previously edematous areas.
(Reijmer et al., 2015)[a]	Cognitive impairment	Probable CAA (n = 29)	LICH (n = 17); other (n = 21)	DVR (cerebellum)	Lower global network efficiency related to higher cortical PiB uptake (p = 0.004)	Structural brain network studied with MRI (DTI). CAA patients with predominantly posterior PiB retention showed lower connection strength in posterior nodes.

CAA: cerebral amyloid angiopathy; HC: healthy control; ICH: intracerebral haemorrhage; L: lobar; rt.-PA: recombinant tissue-type plasminogen activator; WMH: white matter hyperintensities; CSO-PVS: centrum semiovale perivascular spaces; cSS: cortical superficial siderosis; AD = Alzheimer disease; SVCI: subcortical vascular cognitive impairment; CAA-ri: cerebral amyloid angiopathy-related inflammation; pts.: patients; PiB+ and PiB−: PiB positive and PiB negative PET scan, respectively; cSAH: convexity subarachnoid haemorrhage; DTI: diffusion tensor imaging.

[a] PiB.

[b] Florbetapir.

the diagnostic utility of late-phase amyloid PET imaging in CAA, and one additional study dealt with early PiB images as a proxy of brain perfusion (Table 2). Out of these, four have provided data comparing late amyloid uptake in CAA to HCs, and all used PiB (Baron et al., 2014; Gurol et al., 2012; Johnson et al., 2007; Ly et al., 2010a). Three reported a significantly higher whole-cortex PiB uptake in CAA relative to age-matched HCs (Gurol et al., 2012; Johnson et al., 2007; Ly et al., 2010a), while no significant difference was found in one (Baron et al., 2014).

Three studies report the number of subjects with positive or negative PiB scan (Baron et al., 2014; Johnson et al., 2007; Ly et al., 2010a). The reported PiB positivity in probable CAA was 10/11, 6/6 and 7/8, respectively, with corresponding data in HCs of 4/9, 6/15 and 75% (of 22 subjects, i.e., 5 or 6), respectively. Thus, the vast majority (23/25; 92%) of probable CAA patients were PiB+, indicating an excellent sensitivity. In other words, a negative PiB scan rules out CAA with very high confidence. However, specificity was found to be suboptimal due to the frequent occurrence of high PiB uptake in the aged-matched HCs (15 or 16/46, i.e., 1/3), despite normal general cognition (Table 1). This translates into a specificity of ~66%. This incidence of PiB+ in cognitively normal elderly subjects is entirely consistent with the literature and is thought to reflect incipient Alzheimer's disease (Mintun et al., 2006; Rowe et al., 2013). One study only (Ly et al., 2010a) reported PiB data in possible CAA ($n = 4$), with 2 being positive (50%), but without confirmation from a brain biopsy it is uncertain if these patients did have CAA.

A caveat regarding sensitivity for CAA diagnosis is that in patients with suspected CAA, PiB positivity might be incidental, given that the incidence of asymptomatic CAA at autopsy in healthy aged subjects is up to 50% (Kovari et al., 2013). Likewise, due to the frequent co-occurrence of both CAA and AD (Ducharme et al., 2013), patients suspected of CAA might have associated incipient AD accounting for PiB positivity, while conversely healthy controls might harbor incipient CAA. This is particularly important, given the inadequate specificity of amyloid PET. PiB and other amyloid tracers are non-specific imaging markers of Aβ peptide-related parenchymal or cerebrovascular amyloid deposition. Thus, differentiating PiB signal caused by CAA from that caused by other kinds of amyloid deposits is impossible (Klunk et al., 2004; Klunk et al., 2003).

CAA and AD share common molecular mechanisms and certain neuropathological features, but they remain indistinct disease entities, especially when presenting with their sentinel clinical phenotypes. While in AD, CAA can be found in the majority of cases if looked for meticulously, it is usually mild to moderate (Vinters, 2015). By contrast, in CAA with lobar ICH, a well-defined symptomatic phenotype of the disease, especially relevant for amyloid PET studies reviewed here, CAA pathology is severe (usually stage 2 or higher in the Vonsattel scale) (Greenberg and Vonsattel, 1997). In turn, for a definitive neuropathological diagnosis of CAA to be made, a full autopsy is required, typically demonstrating moderate-to-severe cerebrovascular amyloid deposition (Vonsattel stage 2 or more). This is different to “any degree” of vascular amyloid, mainly including mild CAA, which is commonly found to accompany amyloid plaques in AD brains. A recent MRI-neuropathological study compared patients with pathologically proven CAA presenting clinically with or without ICH (Charidimou et al., 2015c). > 90% of pathology samples in both groups had neuritic plaques, whereas neurofibrillary tangles (a hallmark AD lesion) were more commonly present in the patients without ICH (87% vs 42%, $p < 0.0001$) (Charidimou et al., 2015c). Detailed neuropathological information on the Thal and Braak's stages according to age, were not available in this study. In most CAA cases presenting with ICH, the severity degree for amyloid plaques and tangles necessary for a neuropathological diagnosis of AD is not typically met (Hyman et al., 2012). It is important to highlight that amyloid plaques are extremely frequent neuropathologically even in cognitively normal people (around 50% in those > 75 years) (Thal et al., 2002), and thus elderly patients with pure CAA presentations are expected to harbor some amyloid plaques in this context. A large proportion of patients might be situated between these two ends of the amyloid pathologies spectrum. This probably causes some degree of overlap in amyloid PET appearance, yet severe degrees of amyloid deposition affects a fewer proportion of normal people, similar to the case in CAA. Hence, the attempt to differentiate CAA from AD using amyloid PET could be challenging and needs to be based on a number of measures. These include ratios, early PiB update and tau (see below), attempting to dissect out a CAA pattern even on this background of AD-type amyloid deposition and distribution.

Another important aspect that deserves consideration is the role of APOE alleles. APOE ε4 is a known risk factor for AD pathology (Verghese et al., 2011), is associated with a higher likelihood of a positive amyloid PET scan in this setting, as well as with a higher likelihood of lobar microbleeds on blood-sensitive MRI. The role of APOE ε4 has also become more evident by the higher risk of ARIA in immunotherapeutic clinical trials of AD patients. APOE genotype is also among the key genetic determinants of CAA (Greenberg et al., 1996; Greenberg et al., 1995). APOE ε4 enhances cerebrovascular amyloid-β deposition in a dose-dependent manner (Rannikmae et al., 2013). It is hypothesized that APOE ε2 promotes vasculopathic changes (vessel cracking, vessel-within-vessel appearance and fibrinoid necrosis-the most severe stage of CAA) which can in turn result to vessel rupture (Greenberg et al., 1998) including lobar ICH (Charidimou et al., 2015c; Martinez-Ramirez et al., 2014). However, there are no relevant data on how could APOE affect amyloid PET imaging in CAA patients, and this as an area for future investigation. In a memory clinic study, cortical superficial siderosis (a major haemorrhagic CAA biomarker) was associated with other markers of CAA severity, and higher cortical PET-based retention, as well as APOE ε2 presence (Na et al., 2015). How APO-E polymorphism affects amyloid PET in CAA is an important area for future work.

Two additional studies, both using ^{18}F-florbetapir, are relevant to the diagnostic potential of amyloid PET in CAA (Gurol et al., 2016; Raposo et al., 2014a, 2014b). They both compared patients with probable or possible CAA-related symptomatic lobar ICH to patients with symptomatic deep ICH (related to hypertension in Gurol et al.; not stated in Raposo et al) as controls. Both studies found significantly higher global tracer uptake in lobar vs deep ICH, with in addition probable CAA having significantly higher uptake than possible CAA (Raposo et al., 2014a, 2014b). Of note, this difference in tracer uptake between the two groups was present even though 70% of the probable CAA patients were hypertensive, pointing to CAA per se as causing the difference (Gurol et al., 2016). Only Gurol et al. (2016) assessed individual PET positivity (using visual analysis), and reported 10/10 (100%) positivity in lobar ICH vs 1/9 (11%) in deep ICH. These findings are consistent with the excellent sensitivity of PiB relative to HCs detailed above. However, the specificity reported in this study (Gurol et al., 2016) is much higher than previously reported using HCs (see above), yet it would intuitively be expected that elderly subjects with hypertension-related ICH would have similar incidence of incipient AD than HCs. This might be related to the fact that the patients studied in this cohort (Gurol et al., 2016) had a mean age of 67 years, i.e., relatively young. Individual patient analysis is not reported in Raposo et al.'s published abstract (Raposo et al., 2014a, 2014b).

4.1.2. Summary of main findings: regional tracer uptake

As just addressed, the poor specificity of whole-cortex amyloid tracer uptake vs healthy controls affects the diagnostic utility of amyloid PET imaging in CAA. However, if the regional PiB uptake pattern differed between AD and CAA, it might be possible to distinguish these two causes of PiB positivity as a subsequent step in the diagnostic workflow. In other words, in case of PiB positivity relative to HCs, the next step would be to compare the uptake pattern to that present in AD (Fig. 4). As explained in the Results section, all

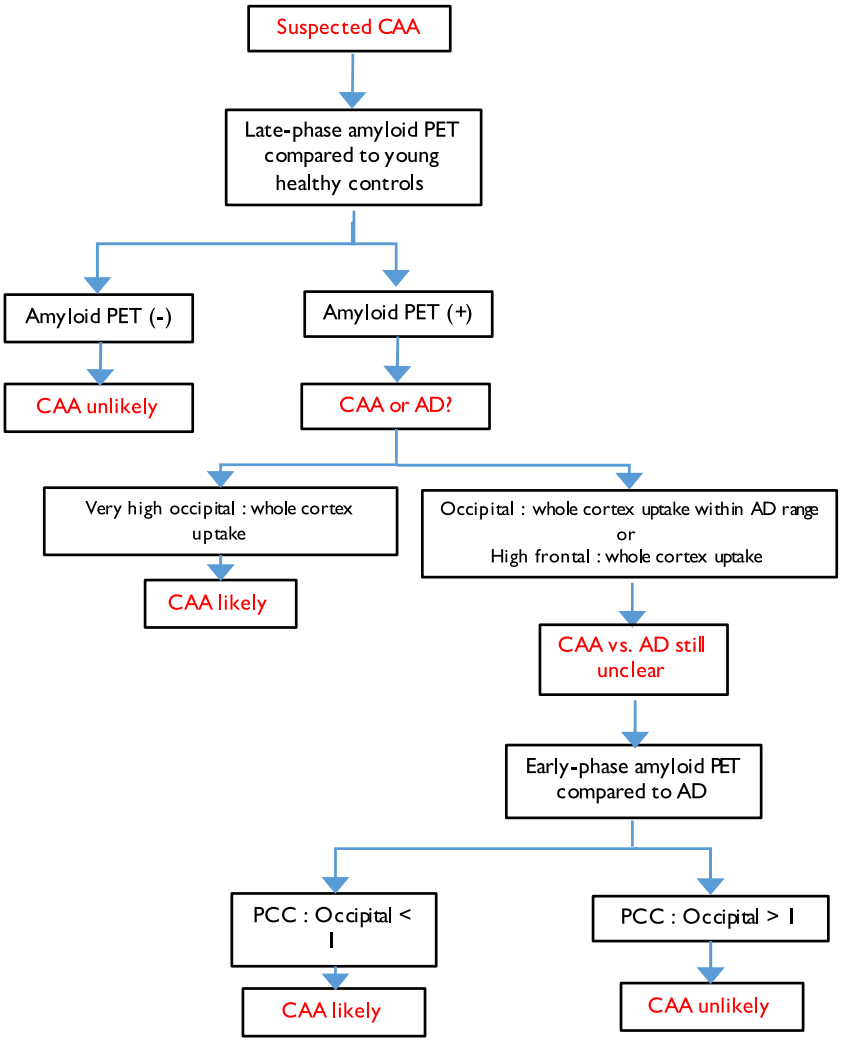

Fig. 4. Diagnostic flow chart algorithm of possible amyloid-PET use in the clinical setting of suspected CAA, based on currently available evidence presented in this review article. This stepwise algorithm is based on three successive steps: i) late-phase amyloid PiB-PET is compared to young controls; ii) if PiB +, then the regional pattern is compared to AD; iii) if still unclear, then the pattern of early PiB images are compared to AD. Note this is a tentative work-flow that is not to be used as evidence-based for routine clinical practice but meant to serve as starting point for future studies.

Table 4
Summary of findings regarding occipital and frontal regional assessment of late-phase amyloid tracer brain uptake.

	Occipital/global ratio	Frontal/global ratio	Occipital/frontal ratio
CAA vs HCs	NS (Baron et al., 2014)	NS (Baron et al., 2014)	N/A
CAA vs HTN-ICH	CAA > HTN-ICH (Gurol et al., 2016)	NS (Gurol et al., 2016)	N/A
CAA vs AD	CAA > AD (Johnson et al., 2007; Ly et al., 2010a)	CAA < AD (Ly et al., 2010a)	CAA > AD (Baron et al., 2014)

CAA: cerebral amyloid angiopathy; HC: healthy controls; NS: no statistically significant difference; > or < : significantly larger or smaller; HTN-ICH: arterial hypertension-related intracerebral haemorrhage; AD: Alzheimer's disease; N/A: not available.

studies so far have focused on the frontal vs occipital contrast. The findings across studies regarding the comparison of the occipital/global, frontal/global and occipital/frontal uptake ratios between probable CAA and HCs or AD samples are summarized in Table 4. As this table shows, only disparate results have been reported so far, precluding any definitive conclusion.

Only Baron et al. (2014) have compared ratios in CAA vs age-matched HCs, reporting no significant difference. However, comparing CAA-related ICH patients to hypertension-related deep ICH subjects, Gurol et al. found a significantly higher occipital/global tracer uptake in CAA (Gurol et al., 2016); the frontal ratio did not significantly differ between the two groups.

Two studies have reported comparison in probable CAA vs probable AD (Johnson et al., 2007; Ly et al., 2010a). In both studies the occipital/whole cortex ratio was significantly lower, and in Ly et al. (2010a) the frontal/whole cortex ratio significantly higher, in AD than CAA. Consistent with the above results, Baron et al. (2014) mentioned in their discussion section a significantly higher calcarine/frontal cortex ratio in CAA as compared to a small sample of AD patients ($n = 7$). Although this finding of an inverted occipital/frontal gradient of amyloid uptake between CAA and AD is important to highlight, especially as it is consistent with the known neuropathological burden in CAA (see above), the data shown in Johnson et al. (2007) and Ly et al. (2010a) (Fig. 3 in both articles) suggest some overlap is present between the two groups, in turn potentially hindering clinical utility. Interestingly, Baron et al. (2014) presented a visual analysis of their PiB + CAA patients according to an 'AD' or 'non-AD' profile, essentially based on occipital cortex uptake, and report 2/3rds of non-AD profile, consistent with the above quantitative data. Relevant to this discussion

is a single-case report with post-mortem assessment of an elderly patient diagnosed in life with probable AD-related cognitive impairment (MMSE = 23) and positive PiB PET with typical regional pattern (i.e., frontal predominance with low occipital uptake), whose pathological diagnosis was CAA without Alzheimer hallmarks (Ducharme et al., 2013). Interestingly, T2-weighted MRI in this patient showed extensive posterior white matter hyperintensities and CSO-PVS, which could have raised the diagnosis of CAA, but T2* imaging was not performed. Unfortunately, one of the larger PiB-PET studies in CAA (Gurol et al., 2013) did not present data on posterior predominance of amyloid tracer retention level in CAA, which would have been useful for further testing this hypothesis. Overall, therefore, the expected difference in anterior/posterior amyloid tracer uptake gradient between CAA and AD is definitely present, however it is unclear whether it has diagnostic significance given the apparent substantial data overlap between the two clinical entities, mirroring the above discussion on neuropathological overlap. Further studies on larger samples directly testing the clinical utility of ratios are warranted at this stage.

To aid the differential diagnosis of CAA vs AD, and based on premises detailed in Methods, a recent study (Farid et al., 2015) assessed the potential use of early PiB images (1–6 min uptake) as a surrogate of resting-state perfusion/metabolism. They predicted that AD and CAA differ in early PiB pattern, with lower occipital and higher posterior cingulate cortex (PCC) uptake in CAA than AD. Consistent with this hypothesis, they report a significantly lower occipital/PCC ratio in CAA than AD. However, there was still some overlap in individual data (Fig. 4). Interestingly, early PiB occipital cortex uptake was significantly lower in CAA patients as compared to HCs, consistent with a recent article reporting a strong trend for reduced MR-based ASL perfusion in the occipital cortex in hereditary CAA with previous lobar ICH (van Opstal et al., 2017). These data suggest that by detecting perfusion-like abnormalities, early-phase PiB-PET might add diagnostic value in combination to late-phase PiB-PET, and particularly help differentiate CAA from Alzheimer's disease. By extension, brain perfusion or metabolism (e.g., FDG PET) imaging using the occipital/PCC ratio might help to clarify the CAA vs AD ambiguity in case of late-phase PiB positivity. Further studies in larger cohorts are needed to ascertain this.

Two additional studies, both using ^{18}F-florbetapir, are relevant to the diagnostic potential of amyloid PET in CAA (Gurol et al., 2016; Raposo et al., 2014a, 2014b). They both compared patients with probable or possible CAA-related symptomatic lobar ICH to patients with symptomatic deep ICH (related to hypertension in Gurol et al.; not stated in Raposo et al.) as controls. Both studies found significantly higher global tracer uptake in lobar vs deep ICH, particularly so in the occipital cortex (Gurol et al., 2016), with probable CAA having significantly higher uptake than possible CAA (Raposo et al., 2014a, 2014b). Of note, this difference in tracer uptake between the two groups was present even though 70% of the probable CAA patients were hypertensive, pointing to CAA per se as causing the difference (Gurol et al., 2016). Only one study (Gurol et al., 2016) assessed individual PET positivity (using visual analysis), and reported 10/10 (100%) positivity in lobar ICH vs 1/9 (11%) in deep ICH. These findings are consistent with the excellent sensitivity of PiB relative to HCs detailed above. However, the specificity reported in this study (Gurol et al., 2016) is much higher than previously reported using HCs, yet it would intuitively be expected that elderly subjects with hypertension-related ICH would have similar incidence of incipient AD than HCs. This might be related to the fact that the patients studied in this cohort (Gurol et al., 2016) had a mean age of 67 years., i.e., relatively young. Individual patient analysis is not reported in Raposo et al.'s published abstract (Raposo et al., 2014a, 2014b).

4.1.3. Methodological issues

The main issue pertains to how to classify subjects as amyloid PET positive or negative. Out of the above six studies, two only used quantitative cut-offs towards objective categorization (Baron et al., 2014; Ly et al., 2010a), and two visual classification only (Gurol et al., 2016; Johnson et al., 2007). One study reports the use of both methods, showing a slight loss of sensitivity with the visual analysis (Baron et al., 2014). The visual method is widely used in clinical practice. However, this binary method of assessment requires a good inter-observer reproducibility and has been described to have worse performance than the quantitative one. In addition, visual analysis doesn't usually assess the regional pattern (e.g., posterior vs anterior predominance), as this would appear even less reliable.

Although the quantitative method is more robust and objective, the whole-cortex tracer uptake threshold approach used to classify a subject as positive or negative raises specific issues. Traditionally calculated cut-offs derived from SUVr are different from, and higher than, those derived from kinetic modelling of the entire time-activity curves since injection time, so-called distribution volume ratios (DVRs) (~1.40 vs ~1.20, respectively). However, the statistical ways to derive them from a control sample (Villeneuve et al., 2015) and the nature of the most appropriate control sample (Baron et al., 2014), have been subject of debate. For instance, if the control sample is small and/or has skewed distribution, deriving a 95% confidence limit might be inadequate. The issue of the nature of the control sample is even more subject to controversy. Thus, if aged-matched HCs are used to determine the cut-off, the inevitable presence of a fraction of PET + subjects will tend to overestimate the cut-off and in turn, to classify truly positive patients as negative. To circumvent this issue, Baron et al. (2014) used a sample of young (< 55 years of age) HC sample, of whom none was visually PiB + as expected from the literature that shows that below this age essentially no HC is PiB + (Mintun et al., 2006; Rodrigue et al., 2012; Vlassenko et al., 2016), consistent with post-mortem data (Thal et al., 2002). Although the effect of age < 55 years on PiB uptake is at best extremely small (Rodrigue et al., 2012), other groups studying AD have used even younger samples (20–30 years old), reporting a 95% UL of 1.07 for DVR (Mormino et al., 2012). Using older control samples, other approaches than the 95% CL that take into account the presence of PiB + subjects use for instance non-parametric iterative outlier exclusion approaches or gaussian mixture (two mixed gaussians) (Villeneuve et al., 2015). A PiB study in healthy subjects using post-mortem as gold-standard found that traditional cut-offs are too conservative, i.e. they classify as negative subjects who are positive at post-mortem (Villeneuve et al., 2015). These authors found that statistical methods that produce less stringent cutoffs provided better concordance with post-mortem than standard 95% CL, and advocated cut-offs of 1.20 and 1.08 for SUVr and DVR, respectively. However, their sub-set of subjects who had both PiB PET and post-mortem had a delay of three years between the two, which might have biased the determination of optimal cut-offs. Regardless, the very concept of a rigid quantitative cut-off is puzzling, and for instance Baron et al. (2014) indicated that the only PiB-probable CAA patient in their sample had a whole cortex PiB DVR of 1.20, just below the cut-off of 1.22, yet was considered 'negative' for the sake of scientific rigor. The same comments apply to quantitative regional values or region-to-global or region-to-region ratios.

Although the regional distribution of vascular amyloid burden in CAA is well described, one study only has so far looked at the regional late uptake values (Baron et al., 2014) as the focus has been on whole cortex average uptake and less so on region/whole cortex or region/region ratios (see above). Yet, it is feasible that focusing on brain regions more likely to be affected in CAA the diagnostic yield of amyloid PET might improve further. However, the way to choose the best combination of brain regions is unclear. Highly sensitive voxel-based approaches such as those developed for FDG PET in AD (Herholz et al., 2002) would be worth exploring. In addition, all studies but one have chosen cerebellar cortex as a reference region (vs pons or cerebellar vermis). Using the cerebellum as reference tissue relies on the assumption that it has only non-specific binding at equilibrium.

Although the cerebellum could be affected by amyloid deposits as part of CAA, it is not entirely clear how often, and to what degree CAA affect the cerebellum, and in all likelihood cerebellar involvement in not very common and might only occur in late and severe stages of the disease (Kovari et al., 2013). Because the cerebellar cortex might be affected by crossed cerebellar diaschisis (Baron et al., 1981), which causes a reduction in perfusion, it is important to consider this possibility in studies of early amyloid tracer uptake. Given that in CAA supratentorial lesions are often bilateral, use of the cerebellar cortex may affect measurements normalized by cerebellum. Accordingly, in Farid et al.'s study of early PiB uptake in CAA, the cerebellar vermis was used as reference tissue (Farid et al., 2015).

Correction for the substantial partial volume effect resulting from the relatively poor spatial resolution of PET is another potential caveat when deriving amyloid cortical tracer uptake values. This is because cortical atrophy, which is present in CAA (Fotiadis et al., 2016), artefactually reduces tracer uptake values in cortical ROIs because of 'spill-out' of radioactivity counts into CSF spaces (Quarantelli et al., 2004). In turn this would result in artificially low tracer uptake values and underestimated true amyloid binding. Although this issue is probably more limited in CAA than in AD, where cortical atrophy is major, it is probably not negligible. So far, only one study (Baron et al., 2014) corrected PiB uptake data for presence of CSF in the cortical ROIs. However, a comparison of the corrected and uncorrected data is not presented.

Although intuitively minimal, the effects of lobar haemorrhage on amyloid tracer retention are unknown. However, no clear difference in late-phase PiB uptake between probable CAA patients with and without history of lobar ICH was mentioned in the two studies that included both types of patients (Gurol et al., 2013; Johnson et al., 2007). Generally, brain regions with previous ICH were removed from the ROI analysis in all studies published in full so far (Table 2). Interestingly, Farid et al. (2015) reported that the significant reduction in early-phase PiB uptake present in CAA as compared to aged-matched HCs became insignificant if data from the hemispheres with previous lobar ICH were removed from the analysis, an effect they attributed to classic remote perfusional/metabolic effects of focal brain lesions, i.e. diaschisis (Baron, 1989; Feeney and Baron, 1986). Nevertheless, this did not affect the difference in occipital/PCC ratio between the CAA and AD groups, which remained highly significant (Farid et al., 2015). Of note, in the previously mentioned ASL perfusion study in hereditary CAA (van Opstal et al., 2017), the areas of previous ICH were discarded from the analysis, and the difference in occipital perfusion between patients and controls was not quite significant after correction for multiple tests; the asymptomatic mutation carriers showed not even a trend for a difference with controls.

4.1.4. Additional points

Heterogeneity in case-mix between the six diagnostic studies reported so far needs mentioning (Table 1). Thus, in two studies (Gurol et al., 2013; Johnson et al., 2007), the CAA sample reported included essentially equal numbers of patients with lobar ICH and other presentations (e.g., seizures, gait problems). Whether this might have biased the findings is unclear insofar as no formal comparison of PiB data between these patient categories is presented in either article.

Another key issue regarding the diagnostic potential of amyloid PET in CAA is that essentially only probable CAA patients have been reported so far. Two studies did include a few patients (8 patients in total) with possible CAA-related lobar ICH (Ly et al., 2010a; Raposo et al., 2014a, 2014b). In one, the two categories were merged for group analyses, which may be problematic, but kept separate when assessing PiB positivity, with 7/8 probable cases being PiB + as compared to 2/4 possible CAA (Ly et al., 2010a). In the other study (Raposo et al., 2014a, 2014b), the probable CAA subgroup ($n = 10$) had higher florbetapir uptake than the possible CAA subgroup (but $n = 4$ only). These limited data would suggest lower amyloid binding in possible CAA, or alternatively that some possible CAA patients in fact did not harbor CAA. Amyloid PET studies in possible CAA are eagerly awaited to assess the potential diagnostic value of amyloid PET at this stage, where formal diagnosis using molecular imaging would be even more useful than in probable CAA. However, in order to allow proper interpretation of the PET findings, prospective long-term follow-up will be necessary to confirm, or disprove, the diagnosis of CAA based on subsequent clinical and imaging events. More generally, the lack of longitudinal amyloid PET studies in CAA so far precludes making any hypothesis regarding the time course of brain amyloid uptake in CAA, specifically how long before the first clinical presentation the amyloid scan becomes positive. In other words, is - as suggested by a recent CSF study (van Etten et al., 2017) - the situation in CAA similar to AD where it is estimated that around 20 years elapse between significant fibrillar amyloid deposition and first symptoms, and where amyloid PET uptake essentially plateaus after the first symptoms surface (Jack et al., 2013; Villemagne et al., 2013), or conversely that in CAA amyloid deposition occurs very soon before, and continues to increase over time after, first symptoms? Studies in symptomatic vs asymptomatic mutation carriers in hereditary CAA, on the model of similar studies in hereditary AD (Bateman et al., 2012), should also provide key data regarding these issues. Finally, a clinically relevant scenario, though relatively rare, is the occurrence of suspected CAA in amyloid-positive patients below the age of 55 (i.e., the lower age limit prescribed by the Boston criteria, see Table 1) in the absence of known gene mutations. No study that far focused on this population.

Two different amyloid PET tracers, namely ^{11}C-PiB and ^{18}F-florbetapir, have so far been used in diagnostic studies in CAA (Table 2). Given that the latter has been validated post-mortem for selective fibrillar Aβ binding and in vivo against the former (Johnson et al., 2007), they should provide similar information, and in turn sensitivity and specificity. The advantage of ^{18}F-florbetapir over ^{11}C-PiB is that thanks to the 2-h half-life of ^{18}F as compared to 20 min for ^{11}C, it is already available commercially (although not yet reimbursed in many countries) so would be used in clinical routine, were amyloid PET to eventually prove its diagnostic utility.

A further point relates to the potential diagnostic value of amyloid PET vs CSF assessment of Aβ 40 vs 42 (and relative to phosphorylated and total tau content) (Piazza et al., 2013; van Etten et al., 2017). For instance, amyloid PET might have added diagnostic value over and above CSF, or vice-versa, or neither. No study on this is available to date, however. The same comment applies to even more understudied potential biomarkers of CAA such CSF Aβ antibodies.

4.2. Mechanistic studies

Because amyloid PET is the only method to date that provides in vivo insight into the regional/local brain density of fibrillar Aβ deposition (as opposed to e.g., CSF which provides a single, indirect global value only), it has the unique potential to decipher the mechanisms involved in the various clinical and radiological features of CAA, more precisely the role of local distribution, intensity and/or pattern of cerebrovascular amyloid deposition in determining these features. This in turn opens new avenues for proper application of future therapies, and for directly monitoring the latter's effects (Sevigny et al., 2016). In practice, using amyloid PET imaging one can rigorously and directly test pre-specified hypotheses on both the quantitative and spatial associations of various indirect markers of CAA-related brain injury with vascular Aβ burden. However, only limited studies have been reported to date, typically with small sample sizes of selected patient populations and with a variety of aims.

Regarding key *haemorrhagic markers* of CAA, two studies focused on lobar CMBs and ICH (Dierksen et al., 2010; Gurol et al., 2012), demonstrating with elegant techniques the spatial correlation between CMBs and PET-based amyloid deposition in shells cross-sectionally, and in areas of new bleeding. These findings suggested that lobar MBs and

ICHs tend to occur in areas with particularly high vascular amyloid burden, via vascular wall fragility. However, some caution is warranted when interpreting these findings. A key limitation is the relatively poor spatial resolution of PET (several mms) compared to MRI-detected CMBs, introducing imprecision in the colocalisation findings. This factor is even more pronounced if the actual neuropathological size of CMBs is considered, being in general 5–20 times smaller than the findings on MRI due to the 'blooming effect' of the susceptibility sequences (Shoamanesh et al., 2011). Quite intriguingly, however, a recent ex vivo 7T MRI-neuropathological study found reduced vascular amyloid burden at sites surrounding CMBs (vs control areas) in CAA brains (van Veluw et al., 2017). The data reviewed here, overall support the expected role of PiB retention as a measure of CAA burden in producing brain injury, but do not inform the actual pathological process leading to blood leaks. Secondly, the CAA cases recruited into these PET studies mainly included cases with relatively large CMBs counts (often > 15) (Dierksen et al., 2010; Gurol et al., 2012), reflecting selection bias. Thus, the relevance of these findings in CAA patients with few lobar CMBs remains unclear and requires replication in larger studies. A potential general implication of the results might be the possibility of preventing or reducing vascular amyloid as a measure to lower the risk of future CAA-related bleeding or other brain injury. This hypothesis has not been directly tested in anti-amyloid immunotherapy CAA trials.

Cortical superficial siderosis (cSS) is emerging as another, and a major, haemorrhagic signature of CAA and the most important predictor of future lobar ICH occurrence, over and above CMBs (Charidimou et al., 2015b). However, cSS has received little attention in PET studies to date. The only available data come from two very small case series (Dhollander et al., 2011; Ly et al., 2015) confirming the role of cSS as a marker of underlying CAA (see Results and Table 3). A study in memory clinic patients (Na et al., 2015), provides the most comprehensive data to date on cSS relationship to amyloid PET imaging. A total of 232 patients with Alzheimer disease–related cognitive impairment and 90 patients with SVCI were rated. cSS was only found in 12 cases (equality distributed in the 2 diagnostic categories), all with positive PET scans, and was associated with indirect biomarkers of CAA presence: higher global PiB retention ratio (relative to patients without cSS), APOE e2 allele, and a strictly lobar microbleeds distribution in multivariate logistic regression analysis (Na et al., 2015). It is important to keep in mind that this memory clinic population, all with cognitive impairment, is not a typical 'pure' symptomatic CAA cohort, hence the generalizability of the results is limited. However, and despite the very small sample size and the high likelihood of amyloid PET burden reflecting AD-type neurodegeneration, the results support the generally accepted notion of cSS being an imaging manifestation of advanced CAA pathology. A well-designed PET-MRI study in a probable CAA clinical population from stroke clinics is needed to further explore the mechanisms of this promising marker, including the global and focal association with amyloid accumulation.

Almost equally as important are the *white matter changes* that occur in CAA, namely white matter hyperintensities on T2/FLAIR MRI (and appearing as leukoaraiosis on pklain CT) and the dilated perivascular space in CSO, as both contribute to the cognitive deterioration, as well probably to the gait impairment, that almost universally develop in CAA survivors over time. In the same vein is the reported association in a single study of white matter hyperintensities and PiB-PET in CAA patients (Gurol et al., 2013), which included 42 non-demented CAA patients, 50 healthy elderly participants and 43 AD/MCI patients. The main pathophysiological argument in the paper is that vascular amyloid burden as captured on PET directly contributes to chronic cerebral ischemia, ultimately giving rise to leukoaraiosis. This interpretation is largely based on the significant correlation found between global PiB retention and leukoaraiosis (rho = 0.52, $p < 0.001$) in the CAA group, but not in the other two control groups. Since this was a cross-sectional study, the CAA group included a mixture of ICH and non-ICH presentations, and measures of cerebral blood flow were not available, it provides only weak support for the underlying hypothesis and mechanistic interpretation. It does however provide evidence for an overall association between total leukoaraiosis burden, a known marker of small vessel disease with heterogeneous pathological basis, and global PET-based amyloid in CAA (as a measure of SVD severity under consideration). More detailed studies are needed to further dissect the regional association between amyloid PET and patterns of leukoaraiosis (e.g. occipital predominance and multiple spots in the white matter), voxel based analysis of cortical amyloid-PET binding and subcortical leukoaraiosis severity, as well as longitudinal analysis over time to prove a causal link between the two measures. In this study, lobar CMBs burden (note: the median CMBs count was 25, somewhat high compared to other CAA cohorts), another putative marker of CAA was also independently associated with leukoaraiosis volume, but other key markers of CAA were not reported, such as cSS and perivascular spaces which could modify the associations under investigation.

MRI-visible PVS in the cerebral white matter, particularly in the CSO, is the latest addition as a neuroimaging CAA signature in the appropriate clinical context (Charidimou et al., 2014; Charidimou et al., 2013b; Martinez-Ramirez et al., 2013; Roher et al., 2003; van Veluw et al., 2016). PVS (also termed Virchow–Robin spaces) are interstitial fluid-filled cavities surrounding small perforating arteries (Ozturk and Aydingoz, 2002) forming potential perivascular channels conceptualized as part of the brain drainage system for interstitial fluid and solutes, including soluble amyloid-β (Carare et al., 2008; Marin-Padilla and Knopman, 2011). It is hypothesized that perivascular spaces are pathologically enlarged when they start to appear on structural MRI, but mechanisms for this assumption remain poorly understood. It is important to clarify that there are no size criteria when perivascular spaces are considered enlarged (see STandards for ReportIng Vascular changes on nEuroimaging (STRIVE)) (Wardlaw et al., 2013). These spaces follow the typical course of penetrating vessels as they go through grey or white matter and hence they appear linear when imaged parallel to the course of the vessel, and round or ovoid, with a diameter generally smaller than 3 mm, when imaged perpendicular to the course of the vessel (Wardlaw et al., 2013).

The association between MRI-visible PVS and CAA might reflect interstitial fluid drainage impairment (Weller et al., 2015), specifically caused by accumulating leptomeningeal and superficial cortical vascular amyloid-β deposition - a central event in the pathophysiology of the disease (Arbel-Ornath et al., 2013a; Hawkes et al., 2011b; Martinez-Ramirez et al., 2013; Roher et al., 2003). Indirect evidence for a role of amyloid load on perivascular drainage impairment came from a PET-based study that suggested that high CSO PVS are associated with higher median cortical PiB retention (Charidimou et al., 2015a). Despite the small sample size, this PET-MRI study demonstrated this hypothesized relationship across a wide range of cerebrovascular amyloid deposition, in both symptomatic CAA-ICH patients and elderly participants, who often harbor asymptomatic CAA (Charidimou et al., 2015a).

No study so far has directly addressed the relationship between the regional distribution of amyloid PET tracer uptake and the severity and pattern of *cognitive impairment* in CAA. In a single center study using DTI-based assessment of brain connectivity, network disturbances were associated with worse cognitive functioning and amyloid load on PET, providing links between vascular amyloid and impairments in white matter connectivity (Reijmer et al., 2015). These brain network alterations in symptomatic CAA patients worsened measurably over just 1.3-year follow-up, progressing from posterior to frontal regions, thought the change in amyloid PET burden during the elapsed time period has not been investigated (Reijmer et al., 2016a). In another study, two patients with CAA-related subacute encephalopathy with inflammatory angiopathy and focal vasogenic edema had positive PiB PET (Carmona-Iragui et al., 2016), suggesting PET might help in the

work-up of this sometimes difficult to diagnose clinical entity.

As already discussed above, serial PET amyloid imaging studies should be applied across the spectrum of the disease and its clinical presentations – in both CAA-ICH and non-ICH 'early' CAA cases or even asymptomatic individuals. Of note, the MRI structural imaging focal lesions represent only the tip of the iceberg of CAA damage, likely reflecting advanced disease. Amyloid PET imaging measures the main feature of CAA pathophysiology – i.e. the severity of amyloid accumulation in the vessels. However, how this process leads on to other vascular changes in of CAA that appear to be instrumental in the pathophysiology of structural MRI lesions, including vessel wall cracking, vasculopathic changes, leptomeningeal vessel vs intracortical vessel amyloid deposition (in leading to cSS vs lobar CMBs) and cortical network dynamics, remains largely unknown. Ample evidence now suggests that CAA is associated with important very early large scale brain microstructural connectivity (Reijmer et al., 2015) and physiological alterations of vascular function/neurovascular coupling (e.g. altered vascular reactivity) (Greenberg et al., 2014). The best established physiological change in individuals with advanced symptomatic CAA is reduced vasodilation to physiologic stimuli. This finding has been demonstrated in studies measuring the functional MRI (fMRI) blood oxygen level-dependent (BOLD) response to visual stimulation (Dumas et al., 2012; Peca et al., 2013; van Opstal et al., 2017). A longitudinal analysis also showed declining amplitude in BOLD response to visual stimulation among CAA patients (Switzer et al., 2016). The same haemodynamic measures were recently found to be impaired (compared to elderly healthy controls) in 12 pre-symptomatic carriers with hereditary cerebral haemorrhage with amyloidosis–Dutch type (van Opstal et al., 2017). These presymptomatic mutation carriers often do not show CMBs, ICH or cSS. These novel findings suggest that vascular reactivity and other physiological markers might be useful early surrogates of vascular amyloid pathology in sporadic CAA (Smith, 2017).

Integrating all the different observations discussed, a well-designed study of serial amyloid PET in combination with fMRI as a measure of cerebrovascular reactivity across the different stages of CAA will be important to perform. CAA is conceptualized as a protein-elimination failure arteriopathy (Carare et al., 2013) setting in motion a self-reinforcing loop (a "feed-forward loop" of reducing drainage efficiency): gradual vascular amyloid-β accumulation leads to impaired vascular physiology, which further increases vascular amyloid-β accumulation (Arbel-Ornath et al., 2013b; Hawkes et al., 2011a). A serial PET-advanced imaging study will demonstrate in vivo the complex interplay and extent to which cerebrovascular amyloid alters vascular physiology and vice versa during follow-up, as well as if these defects trigger clinically relevant haemorrhagic (Zhao et al., 2015) and ischemic brain injury (Reijmer et al., 2016c).

Several studies not included in our systematic review because they did not focus on cohorts of CAA patients, looked at different correlations between SVD imaging markers and PET-based amyloid burden in diverse populations (Kim et al., 2016; Yates et al., 2014; Ye et al., 2015). These data might be informative for presumed mechanisms of SVD MRI markers in general, but it is very challenging to extrapolate them in 'pure CAA' and assess their direct relevance. The main challenge stems from the included populations being only health elderly, memory clinic patients, vascular dementia patients etc. in which codominant Alzheimer's disease pathology in likely high and the clinical context/pretest probability very different compared to CAA patients.

5. Conclusions and future perspectives

Amyloid PET has provided important insights in the clinical relevance and pathophysiological mechanisms of CAA. Our systematic review demonstrates that only small-scale studies have been published so far: (a) for the diagnostic utility, findings seems to be largely consistent, at least in the limited setting that have been tested, but still with several limitations; (b) mechanistic studies provide proof-of-concept data for the direct association between amyloid PET burden and small vessel disease brain injury in CAA, but require validation.

In a nutshell, amyloid PET imaging has 'diagnostic utility' (currently tested only in probable CAA): it helps rule out CAA if negative, whether compared to healthy controls or to hypertensive deep ICH controls. However, if positive, differentiation from underlying incipient AD can be challenging. So far no approach (regional values, ratios, visual assessment) seems sufficient and specific enough to discriminate efficiently CAA from AD, which may in part reflect the neuropathological overlap between these two amyloidopathies. Pending validation, combining early- and late-phase PiB images could potentially prove helpful towards differentiating CAA from AD in case of late PiB positivity, as depicted in the suggested workup algorithm shown in Fig. 4. This algorithm, based on currently available evidence as extensively discussed here, provides an operational framework for future work on, and should be seen only as a step forward towards, the clinical use of amyloid PET in CAA. Prospective studies in isolated lobar ICH ("possible CAA") and in borderline situations (see above) are now warranted. Another potential new avenue in the differentiation between 'pure' CAA and AD/mixed AD-CAA could be dual amyloid and tau PET ligands.

Table 5
Open questions to be addressed in future studies of amyloid PET imaging in CAA.

Diagnosis

- What is the clinical diagnostic yield (sensitivity/specificity) of late-phase amyloid PET in suspected CAA?
  - o In probable CAA-related strictly lobar ICH vs strictly deep non-CAA ICH
  - o In probable CAA-related strictly lobar ICH vs young healthy controls
- Can amyloid PET help in more definite underlying CAA diagnosis in uncertain cases/possible CAA?
  - o Patients with only one lobar ICH (possible CAA)
  - o Mixed ICH cases
  - o CAA Patients presenting without major lobar ICH, especially those with 1–2 lobar CMBs or focal cortical superficial siderosis
- What is the relationship between visual rating of PET +/− scans and amyloid PET cut-offs for diagnostic classification of CAA cases?
- How can early-phase amyloid PET be combined with late phase PET, incorporating different regional patterns of amyloid binding in an evidence-based diagnostic algorithm?
- How does the amyloid PET profile compare to the CSF amyloid and tau profiles?
- Is amyloid PET potentially useful to help diagnose CAA-related inflammation, thus avoiding brain biopsy?
- How amyloid PET imaging may address novel research criteria for CAA and be incorporated with other biomarkers of the disease without the need of neuropathological investigation?

Prognosis

- Is amyloid PET useful for clinical prognosis in CAA patients?
  - o For informing risk stratification of incident/recurrent lobar ICH
  - o For predicting the risk of new onset CAA-related dementia, including post-ICH dementia?
- Can amyloid PET be used as a putative biomarker in CAA therapeutic trials?
  - o For patient selection as a molecular signature of the disease
  - o For monitoring treatment effects (e.g. decrease in amyloid burden)

Mechanisms

- Does amyloid PET hold promise in monitoring the natural history of CAA, i.e. temporal patterns of amyloid accumulation?
- How reliable is amyloid PET in revealing the underlying pathophysiology of the disease, mechanisms, risk factors and rate of amyloid vessel deposition in longitudinal studies?
- How does amyloid PET burden and patterns (globally and focally) relate to the other MRI markers of CAA-related brain damage across the spectrum of clinical presentations (ICH and non-ICH), including cerebral microbleeds, cortical superficial siderosis, cortical microinfarcts and white matter hyperintensities patterns (e.g. posterior predominance)?
- How does amyloid PET help address the AD vs CAA contributions to subcortical vascular cognitive impairment?

Amyloid PET is an important tool to investigate the pathophysiology of CAA and its various manifestations including key MRI lesions and large scale physiological alterations. Amyloid PET imaging should also be useful to select patients for drug trials in CAA, and as an outcome marker to monitor effects of therapy. This will be particularly relevant for early-phase studies aimed at reversing or preventing vascular amyloid deposition. Development of a molecular imaging tracer specific for vascular amyloid can certainly be a milestone in the field and preclinical studies continue to explore possible candidates (Jia et al., 2015, 2014).

Together with the insights provided in our paper, Table 5 summarizes key open questions to be addressed in future studies of amyloid PET imaging in CAA, which will help develop and optimize strategies in the field with the potential to be extended in other forms of SVD.

References

Arbel-Ornath, M., Hudry, E., Eikermann-Haerter, K., Hou, S., Gregory, J.L., Zhao, L., Betensky, R.A., Frosch, M.P., Greenberg, S.M., Bacskai, B.J., 2013a. Interstitial fluid drainage is impaired in ischemic stroke and Alzheimer's disease mouse models. Acta Neuropathol. 126, 353–364.

Arbel-Ornath, M., Hudry, E., Eikermann-Haerter, K., Hou, S., Gregory, J.L., Zhao, L., Betensky, R.A., Frosch, M.P., Greenberg, S.M., Bacskai, B.J., 2013b. Interstitial fluid drainage is impaired in ischemic stroke and Alzheimer's disease mouse models. Acta Neuropathol. 126, 353–364.

Attems, J., Jellinger, K., Thal, D.R., Van Nostrand, W., 2011. Review: sporadic cerebral amyloid angiopathy. Neuropathol. Appl. Neurobiol. 37, 75–93.

Bacskai, B.J., Klunk, W.E., Mathis, C.A., Hyman, B.T., 2002. Imaging amyloid-beta deposits in vivo. J. Cereb. Blood Flow Metab. 22, 1035–1041.

Bacskai, B.J., Frosch, M.P., Freeman, S.H., Raymond, S.B., Augustinack, J.C., Johnson, K.A., Irizarry, M.C., Klunk, W.E., Mathis, C.A., Dekosky, S.T., Greenberg, S.M., Hyman, B.T., Growdon, J.H., 2007. Molecular imaging with Pittsburgh Compound B confirmed at autopsy: a case report. Arch. Neurol. 64, 431–434.

Baron, J.C., 1989. Depression of energy metabolism in distant brain structures: studies with positron emission tomography in stroke patients. Semin. Neurol. 9, 281–285.

Baron, J.C., Bousser, M.G., Comar, D., Castaigne, P., 1981. “Crossed cerebellar diaschisis” in human supratentorial brain infarction. Trans. Am. Neurol. Assoc. 105, 459–461.

Baron, J.C., Farid, K., Dolan, E., Turc, G., Marrapu, S.T., O'Brien, E., Aigbirhio, F.I., Fryer, T.D., Menon, D.K., Warburton, E.A., Hong, Y.T., 2014. Diagnostic utility of amyloid PET in cerebral amyloid angiopathy-related symptomatic intracerebral hemorrhage. J. Cereb. Blood Flow Metab. 34, 753–758.

Bateman, R.J., Xiong, C., Benzinger, T.L., Fagan, A.M., Goate, A., Fox, N.C., Marcus, D.S., Cairns, N.J., Xie, X., Blazey, T.M., Holtzman, D.M., Santacruz, A., Buckles, V., Oliver, A., Moulder, K., Aisen, P.S., Ghetti, B., Klunk, W.E., McDade, E., Martins, R.N., Masters, C.L., Mayeux, R., Ringman, J.M., Rossor, M.N., Schofield, P.R., Sperling, R.A., Salloway, S., Morris, J.C., Dominantly Inherited Alzheimer, N., 2012. Clinical and biomarker changes in dominantly inherited Alzheimer's disease. N. Engl. J. Med. 367, 795–804.

Biffi, A., Halpin, A., Towfighi, A., Gilson, A., Busl, K., Rost, N., Smith, E.E., Greenberg, M.S., Rosand, J., Viswanathan, A., 2010. Aspirin and recurrent intracerebral hemorrhage in cerebral amyloid angiopathy. Neurology 75, 693–698.

Boulouis, G., Charidimou, A., Greenberg, S.M., 2016. Sporadic cerebral amyloid angiopathy: pathophysiology, neuroimaging features, and clinical implications. Semin. Neurol. 36, 233–243.

Carare, R.O., Bernardes-Silva, M., Newman, T.A., Page, A.M., Nicoll, J.A., Perry, V.H., Weller, R.O., 2008. Solutes, but not cells, drain from the brain parenchyma along basement membranes of capillaries and arteries: significance for cerebral amyloid angiopathy and neuroimmunology. Neuropathol. Appl. Neurobiol. 34, 131–144.

Carare, R.O., Hawkes, C.A., Jeffrey, M., Kalaria, R.N., Weller, R.O., 2013. Review: cerebral amyloid angiopathy, prion angiopathy, CADASIL and the spectrum of protein elimination failure angiopathies (PEFA) in neurodegenerative disease with a focus on therapy. Neuropathol. Appl. Neurobiol. 39, 593–611.

Carmona-Iragui, M., Fernandez-Arcos, A., Alcolea, D., Piazza, F., Morenas-Rodriguez, E., Anton-Aguirre, S., Sala, I., Clarimon, J., Dols-Icardo, O., Camacho, V., Sampedro, F., Munuera, J., Nunez-Marin, F., Lleo, A., Fortea, J., Gomez-Anson, B., Blesa, R., 2016. Cerebrospinal fluid anti-amyloid-beta autoantibodies and amyloid PET in cerebral amyloid angiopathy-related inflammation. J. Alzheimers Dis. 50, 1–7.

Charidimou, A., Gang, Q., Werring, D.J., 2012a. Sporadic cerebral amyloid angiopathy revisited: recent insights into pathophysiology and clinical spectrum. J. Neurol. Neurosurg. Psychiatry 83, 124–137.

Charidimou, A., Peeters, A., Fox, Z., Gregoire, S.M., Vandermeeren, Y., Laloux, P., Jager, H.R., Baron, J.C., Werring, D.J., 2012b. Spectrum of transient focal neurological episodes in cerebral amyloid angiopathy: multicentre magnetic resonance imaging cohort study and meta-analysis. Stroke 43, 2324–2330.

Charidimou, A., Baron, J.C., Werring, D.J., 2013a. Transient focal neurological episodes, cerebral amyloid angiopathy, and intracerebral hemorrhage risk: looking beyond TIAs. Int. J. Stroke 8, 105–108.

Charidimou, A., Meegahage, R., Fox, Z., Peeters, A., Vandermeeren, Y., Laloux, P., Baron, J.C., Jager, H.R., Werring, D.J., 2013b. Enlarged perivascular spaces as a marker of underlying arteriopathy in intracerebral haemorrhage: a multicentre MRI cohort study. J. Neurol. Neurosurg. Psychiatry 84, 624–629.

Charidimou, A., Jaunmuktane, Z., Baron, J.C., Burnell, M., Varlet, P., Peeters, A., Xuereb, J., Jager, R., Brandner, S., Werring, D.J., 2014. White matter perivascular spaces: an MRI marker in pathology-proven cerebral amyloid angiopathy? Neurology 82, 57–62.

Charidimou, A., Hong, Y.T., Jager, H.R., Fox, Z., Aigbirhio, F.I., Fryer, T.D., Menon, D.K., Warburton, E.A., Werring, D.J., Baron, J.C., 2015a. White matter perivascular spaces on magnetic resonance imaging: marker of cerebrovascular amyloid burden? Stroke 46, 1707–1709.

Charidimou, A., Linn, J., Vernooij, M.W., Opherk, C., Akoudad, S., Baron, J.C., Greenberg, S.M., Jager, H.R., Werring, D.J., 2015b. Cortical superficial siderosis: detection and clinical significance in cerebral amyloid angiopathy and related conditions. Brain 138, 2126–2139.

Charidimou, A., Martinez-Ramirez, S., Shoamanesh, A., Oliveira-Filho, J., Frosch, M., Vashkevich, A., Ayres, A., Rosand, J., Gurol, M.E., Greenberg, S.M., Viswanathan, A., 2015c. Cerebral amyloid angiopathy with and without hemorrhage: evidence for different disease phenotypes. Neurology 84, 1206–1212.

Charidimou, A., Nicoll, J.A., McCarron, M.O., 2015d. Thrombolysis-related intracerebral hemorrhage and cerebral amyloid angiopathy: accumulating evidence. Front. Neurol. 6, 99.

Dhollander, I., Nelissen, N., Van Laere, K., Peeters, D., Demaerel, P., Van Paesschen, W., Thijs, V., Vandenberghe, R., 2011. In vivo amyloid imaging in cortical superficial siderosis. J. Neurol. Neurosurg. Psychiatry 82, 469–471.

Dierksen, G.A., Skehan, M.E., Khan, M.A., Jeng, J., Nandigam, R.N., Becker, J.A., Kumar, A., Neal, K.L., Betensky, R.A., Frosch, M.P., Rosand, J., Johnson, K.A., Viswanathan, A., Salat, D.H., Greenberg, S.M., 2010. Spatial relation between microbleeds and amyloid deposits in amyloid angiopathy. Ann. Neurol. 68, 545–548.

Ducharme, S., Guiot, M.C., Nikelski, J., Chertkow, H., 2013. Does a positive Pittsburgh compound B scan in a patient with dementia equal Alzheimer disease? JAMA Neurol. 70, 912–914.

Dumas, A., Dierksen, G.A., Gurol, M.E., Halpin, A., Martinez-Ramirez, S., Schwab, K., Rosand, J., Viswanathan, A., Salat, D.H., Polimeni, J.R., Greenberg, S.M., 2012. Functional magnetic resonance imaging detection of vascular reactivity in cerebral amyloid angiopathy. Ann. Neurol. 72, 76–81.

van Etten, E.S., Verbeek, M.M., van der Grond, J., Zielman, R., van Rooden, S., van Zwet, E.W., van Opstal, A.M., Haan, J., Greenberg, S.M., van Buchem, M.A., Wermer, M.J., Terwindt, G.M., 2017. Beta-amyloid in CSF: biomarker for preclinical cerebral amyloid angiopathy. Neurology 88, 169–176.

Farid, K., Hong, Y.T., Aigbirhio, F.I., Fryer, T.D., Menon, D.K., Warburton, E.A., Baron, J.C., 2015. Early-phase 11C-PiB PET in amyloid angiopathy-related symptomatic cerebral hemorrhage: potential diagnostic value? PLoS One 10, e0139926.

Feeney, D.M., Baron, J.C., 1986. Diaschisis. Stroke 17, 817–830.

Forsberg, A., Engler, H., Blomquist, G., Langstrom, B., Nordberg, A., 2012. The use of PIB-PET as a dual pathological and functional biomarker in AD. Biochim. Biophys. Acta 1822, 380–385.

Fotiadis, P., van Rooden, S., van der Grond, J., Schultz, A., Martinez-Ramirez, S., Auriel, E., Reijmer, Y., van Opstal, A.M., Ayres, A., Schwab, K.M., Alzheimer's Disease Neuroimaging Initiative, A., Hedden, T., Rosand, J., Viswanathan, A., Wermer, M., Terwindt, G.M., Sperling, R.A., Polimeni, J.R., Johnson, K.A., van Buchem, M.A., Greenberg, S.M., Gurol, M.E., 2016. Cortical atrophy in patients with cerebral amyloid angiopathy: a case-control study. Lancet Neurol. 15, 811–819.

Greenberg, S.M., Vonsattel, J.P., 1997. Diagnosis of cerebral amyloid angiopathy. Sensitivity and specificity of cortical biopsy. Stroke 28, 1418–1422.

Greenberg, S.M., Rebeck, G.W., Vonsattel, J.P., Gomez-Isla, T., Hyman, B.T., 1995. Apolipoprotein E epsilon 4 and cerebral hemorrhage associated with amyloid angiopathy. Ann. Neurol. 38, 254–259.

Greenberg, S.M., Briggs, M.E., Hyman, B.T., Kokoris, G.J., Takis, C., Kanter, D.S., Kase, C.S., Pessin, M.S., 1996. Apolipoprotein E epsilon 4 is associated with the presence and earlier onset of hemorrhage in cerebral amyloid angiopathy. Stroke 27, 1333–1337.

Greenberg, S.M., Vonsattel, J.P., Segal, A.Z., Chiu, R.I., Clatworthy, A.E., Liao, A., Hyman, B.T., Rebeck, G.W., 1998. Association of apolipoprotein E epsilon2 and vasculopathy in cerebral amyloid angiopathy. Neurology 50, 961–965.

Greenberg, S.M., Grabowski, T., Gurol, M.E., Skehan, M.E., Nandigam, R.N., Becker, J.A., Garcia-Alloza, M., Prada, C., Frosch, M.P., Rosand, J., Viswanathan, A., Smith, E.E., Johnson, K.A., 2008. Detection of isolated cerebrovascular beta-amyloid with Pittsburgh compound B. Ann. Neurol. 64, 587–591.

Greenberg, S.M., Salman, R.A., Biessels, G.J., van Buchem, M., Cordonnier, C., Lee, J.M., Montaner, J., Schneider, J.A., Smith, E.E., Vernooij, M., Werring, D.J., 2014. Outcome markers for clinical trials in cerebral amyloid angiopathy. Lancet Neurol. 13, 419–428.

Gurol, M.E., Dierksen, G., Betensky, R., Gidicsin, C., Halpin, A., Becker, A., Carmasin, J., Ayres, A., Schwab, K., Viswanathan, A., Salat, D., Rosand, J., Johnson, K.A., Greenberg, S.M., 2012. Predicting sites of new hemorrhage with amyloid imaging in cerebral amyloid angiopathy. Neurology 79, 320–326.

Gurol, M.E., Viswanathan, A., Gidicsin, C., Hedden, T., Martinez-Ramirez, S., Dumas, A., Vashkevich, A., Ayres, A.M., Auriel, E., van Etten, E., Becker, A., Carmasin, J., Schwab, K., Rosand, J., Johnson, K.A., Greenberg, S.M., 2013. Cerebral amyloid angiopathy burden associated with leukoaraiosis: a positron emission tomography/magnetic resonance imaging study. Ann. Neurol. 73, 529–536.

Gurol, M.E., Becker, J.A., Fotiadis, P., Riley, G., Schwab, K., Johnson, K.A., Greenberg, S.M., 2016. Florbetapir-PET to diagnose cerebral amyloid angiopathy: a prospective study. Neurology 87, 2043–2049.

Hawkes, C.A., Hartig, W., Kacza, J., Schliebs, R., Weller, R.O., Nicoll, J.A., Carare, R.O., 2011a. Perivascular drainage of solutes is impaired in the ageing mouse brain and in the presence of cerebral amyloid angiopathy. Acta Neuropathol. 121, 431–443.

Hawkes, C.A., Hartig, W., Kacza, J., Schliebs, R., Weller, R.O., Nicoll, J.A., Carare, R.O.,

2011b. Perivascular drainage of solutes is impaired in the ageing mouse brain and in the presence of cerebral amyloid angiopathy. Acta Neuropathol. 121, 431–443.
Herholz, K., Salmon, E., Perani, D., Baron, J.C., Holthoff, V., Frolich, L., Schonknecht, P., Ito, K., Mielke, R., Kalbe, E., Zundorf, G., Delbeuck, X., Pelati, O., Anchisi, D., Fazio, F., Kerrouche, N., Desgranges, B., Eustache, F., Beuthien-Baumann, B., Menzel, C., Schroder, J., Kato, T., Arahata, Y., Henze, M., Heiss, W.D., 2002. Discrimination between Alzheimer dementia and controls by automated analysis of multicenter FDG PET. NeuroImage 17, 302–316.
Hyman, B.T., Phelps, C.H., Beach, T.G., Bigio, E.H., Cairns, N.J., Carrillo, M.C., Dickson, D.W., Duyckaerts, C., Frosch, M.P., Masliah, E., Mirra, S.S., Nelson, P.T., Schneider, J.A., Thal, D.R., Thies, B., Trojanowski, J.Q., Vinters, H.V., Montine, T.J., 2012. National Institute on Aging-Alzheimer's Association guidelines for the neuropathologic assessment of Alzheimer's disease. Alzheimers Dement. 8, 1–13.
Jack Jr., C.R., Knopman, D.S., Jagust, W.J., Petersen, R.C., Weiner, M.W., Aisen, P.S., Shaw, L.M., Vemuri, P., Wiste, H.J., Weigand, S.D., Lesnick, T.G., Pankratz, V.S., Donohue, M.C., Trojanowski, J.Q., 2013. Tracking pathophysiological processes in Alzheimer's disease: an updated hypothetical model of dynamic biomarkers. Lancet Neurol. 12, 207–216.
Jellinger, K.A., 2002. Alzheimer disease and cerebrovascular pathology: an update. J. Neural Transm. 109, 813–836.
Jia, J., Cui, M., Dai, J., Wang, X., Ding, Y., Jiaa, H., Liua, B., 2014. 99mTc-labeled benzothiazole and stilbene derivatives as imaging agents for Aβ plaques in cerebral amyloid angiopathy. Med. Chem. Commun. 5, 153–158.
Jia, J., Cui, M., Dai, J., Liu, B., 2015. (99m)Tc(CO)3-labeled benzothiazole derivatives preferentially bind cerebrovascular amyloid: potential use as imaging agents for cerebral amyloid angiopathy. Mol. Pharm. 12, 2937–2946.
Johnson, K.A., Gregas, M., Becker, J.A., Kinnecom, C., Salat, D.H., Moran, E.K., Smith, E.E., Rosand, J., Rentz, D.M., Klunk, W.E., Mathis, C.A., Price, J.C., Dekosky, S.T., Fischman, A.J., Greenberg, S.M., 2007. Imaging of amyloid burden and distribution in cerebral amyloid angiopathy. Ann. Neurol. 62, 229–234.
Kalaria, R.N., Ballard, C., 1999. Overlap between pathology of Alzheimer disease and vascular dementia. Alzheimer Dis. Assoc. Disord. 13 (Suppl. 3), S115–S123.
Keage, H.A., Carare, R.O., Friedland, R.P., Ince, P.G., Love, S., Nicoll, J.A., Wharton, S.B., Weller, R.O., Brayne, C., 2009. Population studies of sporadic cerebral amyloid angiopathy and dementia: a systematic review. BMC Neurol. 9, 3.
Kim, Y.J., Kim, H.J., Park, J.H., Kim, S., Woo, S.Y., Kwak, K.C., Lee, J.M., Jung, N.Y., Kim, J.S., Choe, Y.S., Lee, K.H., Moon, S.H., Lee, J.H., Kim, Y.J., Werring, D.J., Na, D.L., Seo, S.W., 2016. Synergistic effects of longitudinal amyloid and vascular changes on lobar microbleeds. Neurology 87, 1575–1582.
Klunk, W.E., Wang, Y., Huang, G.F., Debnath, M.L., Holt, D.P., Shao, L., Hamilton, R.L., Ikonomovic, M.D., DeKosky, S.T., Mathis, C.A., 2003. The binding of 2-(4′-methylaminophenyl)benzothiazole to postmortem brain homogenates is dominated by the amyloid component. J. Neurosci. 23, 2086–2092.
Klunk, W.E., Engler, H., Nordberg, A., Wang, Y., Blomqvist, G., Holt, D.P., Bergstrom, M., Savitcheva, I., Huang, G.F., Estrada, S., Ausen, B., Debnath, M.L., Barletta, J., Price, J.C., Sandell, J., Lopresti, B.J., Wall, A., Koivisto, P., Antoni, G., Mathis, C.A., Langstrom, B., 2004. Imaging brain amyloid in Alzheimer's disease with Pittsburgh Compound-B. Ann. Neurol. 55, 306–319.
Knudsen, K.A., Rosand, J., Karluk, D., Greenberg, S.M., 2001. Clinical diagnosis of cerebral amyloid angiopathy: validation of the Boston criteria. Neurology 56, 537–539.
Kovari, E., Herrmann, F.R., Hof, P.R., Bouras, C., 2013. The relationship between cerebral amyloid angiopathy and cortical microinfarcts in brain ageing and Alzheimer's disease. Neuropathol. Appl. Neurobiol. 39, 498–509.
Linn, J., Halpin, A., Demaerel, P., Ruhland, J., Giese, A.D., Dichgans, M., van Buchem, M.A., Bruckmann, H., Greenberg, S.M., 2010. Prevalence of superficial siderosis in patients with cerebral amyloid angiopathy. Neurology 74, 1346–1350.
Love, S., Chalmers, K., Ince, P., Esiri, M., Attems, J., Jellinger, K., Yamada, M., McCarron, M., Minett, T., Matthews, F., Greenberg, S., Mann, D., Kehoe, P.G., 2014. Development, appraisal, validation and implementation of a consensus protocol for the assessment of cerebral amyloid angiopathy in post-mortem brain tissue. Am. J. Neurodegener. Dis. 3, 19–32.
Ly, J.V., Donnan, G.A., Villemagne, V.L., Zavala, J.A., Ma, H., O'Keefe, G., Gong, S.J., Gunawan, R.M., Saunder, T., Ackerman, U., Tochon-Danguy, H., Churilov, L., Phan, T.G., Rowe, C.C., 2010a. 11C-PIB binding is increased in patients with cerebral amyloid angiopathy-related hemorrhage. Neurology 74, 487–493.
Ly, J.V., Rowe, C.C., Villemagne, V.L., Zavala, J.A., Ma, H., O'Keefe, G., Gong, S.J., Gunawan, R., Churilov, L., Saunder, T., Ackerman, U., Tochon-Danguy, H., Donnan, G.A., 2010b. Cerebral beta-amyloid detected by Pittsburgh compound B positron emission topography predisposes to recombinant tissue plasminogen activator-related hemorrhage. Ann. Neurol. 68, 959–962.
Ly, J.V., Singhal, S., Rowe, C.C., Kempster, P., Bower, S., Phan, T.G., 2015. Convexity subarachnoid hemorrhage with PiB positive pet scans: clinical features and prognosis. J. Neuroimaging 25, 420–429.
Marin-Padilla, M., Knopman, D.S., 2011. Developmental aspects of the intracerebral microvasculature and perivascular spaces: insights into brain response to late-life diseases. J. Neuropathol. Exp. Neurol. 70, 1060–1069.
Martinez-Ramirez, S., Pontes-Neto, O.M., Dumas, A.P., Auriel, E., Halpin, A., Quimby, M., Gurol, M.E., Greenberg, S.M., Viswanathan, A., 2013. Topography of dilated perivascular spaces in subjects from a memory clinic cohort. Neurology 80, 1551–1556.
Martinez-Ramirez, S., Romero, J.R., Shoamanesh, A., McKee, A.C., Van Etten, E., Pontes-Neto, O., Macklin, E.A., Ayres, A., Auriel, E., Himali, J.J., Beiser, A.S., DeCarli, C., Stein, T.D., Alvarez, V.E., Frosch, M.P., Rosand, J., Greenberg, S.M., Gurol, M.E., Seshadri, S., Viswanathan, A., 2015. Diagnostic value of lobar microbleeds in individuals without intracerebral hemorrhage. Alzheimers Dement. 11, 1480–1488.
Mattila, O.S., Sairanen, T., Laakso, E., Paetau, A., Tanskanen, M., Lindsberg, P.J., 2015. Cerebral amyloid angiopathy related hemorrhage after stroke thrombolysis: case report and literature review. Neuropathology 35, 70–74.
Mintun, M.A., Larossa, G.N., Sheline, Y.I., Dence, C.S., Lee, S.Y., Mach, R.H., Klunk, W.E., Mathis, C.A., DeKosky, S.T., Morris, J.C., 2006. [11C]PIB in a nondemented population: potential antecedent marker of Alzheimer disease. Neurology 67, 446–452.
Mormino, E.C., Brandel, M.G., Madison, C.M., Rabinovici, G.D., Marks, S., Baker, S.L., Jagust, W.J., 2012. Not quite PIB-positive, not quite PIB-negative: slight PIB elevations in elderly normal control subjects are biologically relevant. NeuroImage 59, 1152–1160.
Na, H.K., Park, J.H., Kim, J.H., Kim, H.J., Kim, S.T., Werring, D.J., Seo, S.W., Na, D.L., 2015. Cortical superficial siderosis: a marker of vascular amyloid in patients with cognitive impairment. Neurology 84, 849–855.
van Opstal, A.M., van Rooden, S., van Harten, T., Ghariq, E., Labadie, G., Fotiadis, P., Gurol, M.E., Terwindt, G.M., Wermer, M.J., van Buchem, M.A., Greenberg, S.M., van der Grond, J., 2017. Cerebrovascular function in presymptomatic and symptomatic individuals with hereditary cerebral amyloid angiopathy: a case-control study. Lancet Neurol. 16 (2), 115–122 (Feb).
Ozturk, M.H., Aydingoz, U., 2002. Comparison of MR signal intensities of cerebral perivascular (Virchow-Robin) and subarachnoid spaces. J. Comput. Assist. Tomogr. 26, 902–904.
Peca, S., McCreary, C.R., Donaldson, E., Kumarpillai, G., Shobha, N., Sanchez, K., Charlton, A., Steinback, C.D., Beaudin, A.E., Fluck, D., Pillay, N., Fick, G.H., Poulin, M.J., Frayne, R., Goodyear, B.G., Smith, E.E., 2013. Neurovascular decoupling is associated with severity of cerebral amyloid angiopathy. Neurology 81, 1659–1665.
Piazza, F., Greenberg, S.M., Savoiardo, M., Gardinetti, M., Chiapparini, L., Raicher, I., Nitrini, R., Sakaguchi, H., Brioschi, M., Billo, G., Colombo, A., Lanzani, F., Piscosquito, G., Carriero, M.R., Giaccone, G., Tagliavini, F., Ferrarese, C., DiFrancesco, J.C., 2013. Anti-amyloid beta autoantibodies in cerebral amyloid angiopathy-related inflammation: implications for amyloid-modifying therapies. Ann. Neurol. 73, 449–458.
Quarantelli, M., Berkouk, K., Prinster, A., Landeau, B., Svarer, C., Balkay, L., Alfano, B., Brunetti, A., Baron, J.C., Salvatore, M., 2004. Integrated software for the analysis of brain PET/SPECT studies with partial-volume-effect correction. J. Nucl. Med. 45, 192–201.
Rannikmae, K., Samarasekera, N., Martinez-Gonzalez, N.A., Al-Shahi Salman, R., Sudlow, C.L., 2013. Genetics of cerebral amyloid angiopathy: systematic review and meta-analysis. J. Neurol. Neurosurg. Psychiatry 84, 901–908.
Raposo, N., Planton, M., Peran, P., Payoux, P., Bonneville, F., Albucher, J.F., Olivot, J.M., Hitzel, A., Chollet, F., Pariente, J., 2014a. Florbetapir imaging in deep and cerebral amyloid angiopathy related intracerebral hemorrhages. In: 9th World Stroke Congress Poster 398, Istanbul, Turkey.
Raposo, N., Planton, M., Peran, P., Payoux, P., Bonneville, F., Albucher, J.F., Olivot, J.M., Hitzel, A., Chollet, F., Pariente, J., 2014b. Florbetapir imaging in deep and cerebral amyloid angiopathy related intracerebral hemorrhages. In: 9th World Stroke Congress, Istanbul, Turkey, (p. Poster 398).
Reijmer, Y.D., Fotiadis, P., Martinez-Ramirez, S., Salat, D.H., Schultz, A., Shoamanesh, A., Ayres, A.M., Vashkevich, A., Rosas, D., Schwab, K., Leemans, A., Biessels, G.J., Rosand, J., Johnson, K.A., Viswanathan, A., Gurol, M.E., Greenberg, S.M., 2015. Structural network alterations and neurological dysfunction in cerebral amyloid angiopathy. Brain 138, 179–188.
Reijmer, Y., Fotiadis, P., Martinez-Ramirez, S., Ayres, M.A., Vashkevich, A., Schwab, K., Rosand, J., Viswanathan, A., Gurol, M.E., Greenberg, M.S., 2016a. Progression of brain network alterations in patients with cerebral amyloid angiopathy. In: International Stroke Conference. Stroke, Los Angeles, pp. A:124.
Reijmer, Y.D., Fotiadis, P., Riley, G.A., Xiong, L., Charidimou, A., Boulouis, G., Ayres, A.M., Schwab, K., Rosand, J., Gurol, M.E., Viswanathan, A., Greenberg, S.M., 2016b. Progression of brain network alterations in cerebral amyloid angiopathy. Stroke 47, 2470–2475.
Reijmer, Y.D., van Veluw, S.J., Greenberg, S.M., 2016c. Ischemic brain injury in cerebral amyloid angiopathy. J. Cereb. Blood Flow Metab. 36, 40–54.
Rodrigue, K.M., Kennedy, K.M., Devous Sr., M.D., Rieck, J.R., Hebrank, A.C., Diaz-Arrastia, R., Mathews, D., Park, D.C., 2012. Beta-amyloid burden in healthy aging: regional distribution and cognitive consequences. Neurology 78, 387–395.
Rodriguez-Vieitez, E., Leuzy, A., Chiotis, K., Saint-Aubert, L., Wall, A., Nordberg, A., 2017. Comparability of [18F]THK5317 and [11C]PIB blood flow proxy images with [18F]FDG positron emission tomography in Alzheimer's disease. J. Cereb. Blood Flow Metab. 37, 740–749.
Roher, A.E., Kuo, Y.M., Esh, C., Knebel, C., Weiss, N., Kalback, W., Luehrs, D.C., Childress, J.L., Beach, T.G., Weller, R.O., Kokjohn, T.A., 2003. Cortical and leptomeningeal cerebrovascular amyloid and white matter pathology in Alzheimer's disease. Mol. Med. 9, 112–122.
Rosand, J., Muzikansky, A., Kumar, A., Wisco, J.J., Smith, E.E., Betensky, R.A., Greenberg, S.M., 2005. Spatial clustering of hemorrhages in probable cerebral amyloid angiopathy. Ann. Neurol. 58, 459–462.
Rostomian, A.H., Madison, C., Rabinovici, G.D., Jagust, W.J., 2011. Early 11C-PIB frames and 18F-FDG PET measures are comparable: a study validated in a cohort of AD and FTLD patients. J. Nucl. Med. 52, 173–179.
Rowe, C.C., Bourgeat, P., Ellis, K.A., Brown, B., Lim, Y.Y., Mulligan, R., Jones, G., Maruff, P., Woodward, M., Price, R., Robins, P., Tochon-Danguy, H., O'Keefe, G., Pike, K.E., Yates, P., Szoeke, C., Salvado, O., Macaulay, S.L., O'Meara, T., Head, R., Cobiac, L., Savage, G., Martins, R., Masters, C.L., Ames, D., Villemagne, V.L., 2013. Predicting Alzheimer disease with beta-amyloid imaging: results from the Australian imaging, biomarkers, and lifestyle study of ageing. Ann. Neurol. 74, 905–913.
Sekijima, Y., Yazaki, M., Oguchi, K., Ezawa, N., Yoshinaga, T., Yamada, M., Yahikozawa,

H., Watanabe, M., Kametani, F., Ikeda, S., 2016. Cerebral amyloid angiopathy in posttransplant patients with hereditary ATTR amyloidosis. Neurology 87, 773–781.
Sevigny, J., Chiao, P., Bussiere, T., Weinreb, P.H., Williams, L., Maier, M., Dunstan, R., Salloway, S., Chen, T., Ling, Y., O'Gorman, J., Qian, F., Arastu, M., Li, M., Chollate, S., Brennan, M.S., Quintero-Monzon, O., Scannevin, R.H., Arnold, H.M., Engber, T., Rhodes, K., Ferrero, J., Hang, Y., Mikulskis, A., Grimm, J., Hock, C., Nitsch, R.M., Sandrock, A., 2016. The antibody aducanumab reduces Abeta plaques in Alzheimer's disease. Nature 537, 50–56.
Shoamanesh, A., Kwok, C.S., Benavente, O., 2011. Cerebral microbleeds: histopathological correlation of neuroimaging. Cerebrovasc. Dis. 32, 528–534.
Shoamanesh, A., Martinez-Ramirez, S., Oliveira-Filho, J., Reijmer, Y., Falcone, G.J., Ayres, A., Schwab, K., Goldstein, J.N., Rosand, J., Gurol, M.E., Viswanathan, A., Greenberg, S.M., 2014. Interrelationship of superficial siderosis and microbleeds in cerebral amyloid angiopathy. Neurology 83, 1838–1843.
Smith, E.E., 2017. Defining early CAA: insights from a rare monogenic disorder. Lancet Neurol. 16 (2), 98–99 (Feb).
Switzer, A.R., McCreary, C., Batool, S., Stafford, R.B., Frayne, R., Goodyear, B.G., Smith, E.E., 2016. Longitudinal decrease in blood oxygenation level dependent response in cerebral amyloid angiopathy. Neuroimage Clin. 11, 461–467.
Thal, D.R., Rub, U., Orantes, M., Braak, H., 2002. Phases of A beta-deposition in the human brain and its relevance for the development of AD. Neurology 58, 1791–1800.
van Veluw, S.J., Biessels, G.J., Bouvy, W.H., Spliet, W.G., Zwanenburg, J.J., Luijten, P.R., Macklin, E.A., Rozemuller, A.J., Gurol, M.E., Greenberg, S.M., Viswanathan, A., Martinez-Ramirez, S., 2016. Cerebral amyloid angiopathy severity is linked to dilation of juxtacortical perivascular spaces. J. Cereb. Blood Flow Metab. 36, 576–580.
van Veluw, S.J., Kuijf, H.J., Charidimou, A., Viswanathan, A., Biessels, G.J., Rozemuller, A.J., Frosch, M.P., Greenberg, S.M., 2017. Reduced vascular amyloid burden at microhemorrhage sites in cerebral amyloid angiopathy. Acta Neuropathol. 133 (3), 409–415.
Verghese, P.B., Castellano, J.M., Holtzman, D.M., 2011. Apolipoprotein E in Alzheimer's disease and other neurological disorders. Lancet Neurol. 10, 241–252.
Villemagne, V.L., Burnham, S., Bourgeat, P., Brown, B., Ellis, K.A., Salvado, O., Szoeke, C., Macaulay, S.L., Martins, R., Maruff, P., Ames, D., Rowe, C.C., Masters, C.L., Australian Imaging, B., Lifestyle Research, G., 2013. Amyloid beta deposition, neurodegeneration, and cognitive decline in sporadic Alzheimer's disease: a prospective cohort study. Lancet Neurol. 12, 357–367.
Villeneuve, S., Rabinovici, G.D., Cohn-Sheehy, B.I., Madison, C., Ayakta, N., Ghosh, P.M., La Joie, R., Arthur-Bentil, S.K., Vogel, J.W., Marks, S.M., Lehmann, M., Rosen, H.J., Reed, B., Olichney, J., Boxer, A.L., Miller, B.L., Borys, E., Jin, L.W., Huang, E.J., Grinberg, L.T., DeCarli, C., Seeley, W.W., Jagust, W., 2015. Existing Pittsburgh compound-B positron emission tomography thresholds are too high: statistical and pathological evaluation. Brain 138, 2020–2033.
Vinters, H.V., 1987. Cerebral amyloid angiopathy. A critical review. Stroke 18, 311–324.
Vinters, H.V., 2015. Emerging concepts in Alzheimer's disease. Annu. Rev. Pathol. 10, 291–319.
Vinters, H.V., Gilbert, J.J., 1983. Cerebral amyloid angiopathy: incidence and complications in the aging brain. II. The distribution of amyloid vascular changes. Stroke 14, 924–928.
Viswanathan, A., Greenberg, S.M., 2011. Cerebral amyloid angiopathy in the elderly. Ann. Neurol. 70, 871–880.
Vlassenko, A.G., McCue, L., Jasielec, M.S., Su, Y., Gordon, B.A., Xiong, C., Holtzman, D.M., Benzinger, T.L., Morris, J.C., Fagan, A.M., 2016. Imaging and cerebrospinal fluid biomarkers in early preclinical Alzheimer disease. Ann. Neurol. 80, 379–387.
Wardlaw, J.M., Smith, E.E., Biessels, G.J., Cordonnier, C., Fazekas, F., Frayne, R., Lindley, R.I., O'Brien, J.T., Barkhof, F., Benavente, O.R., Black, S.E., Brayne, C., Breteler, M., Chabriat, H., Decarli, C., de Leeuw, F.E., Doubal, F., Duering, M., Fox, N.C., Greenberg, S., Hachinski, V., Kilimann, I., Mok, V., Oostenbrugge, R., Pantoni, L., Speck, O., Stephan, B.C., Teipel, S., Viswanathan, A., Werring, D., Chen, C., Smith, C., van Buchem, M., Norrving, B., Gorelick, P.B., Dichgans, M., 2013. Neuroimaging standards for research into small vessel disease and its contribution to ageing and neurodegeneration. Lancet Neurol. 12, 822–838.
Weller, R.O., Hawkes, C.A., Kalaria, R.N., Werring, D.J., Carare, R.O., 2015. White matter changes in dementia: role of impaired drainage of interstitial fluid. Brain Pathol. 25, 63–78.
Yates, P.A., Desmond, P.M., Phal, P.M., Steward, C., Szoeke, C., Salvado, O., Ellis, K.A., Martins, R.N., Masters, C.L., Ames, D., Villemagne, V.L., Rowe, C.C., A. R. Group, 2014. Incidence of cerebral microbleeds in preclinical Alzheimer disease. Neurology 82, 1266–1273.
Ye, B.S., Seo, S.W., Kim, J.H., Kim, G.H., Cho, H., Noh, Y., Kim, H.J., Yoon, C.W., Woo, S.Y., Kim, S.H., Park, H.K., Kim, S.T., Choe, Y.S., Lee, K.H., Kim, J.S., Oh, S.J., Kim, C., Weiner, M., Lee, J.H., Na, D.L., 2015. Effects of amyloid and vascular markers on cognitive decline in subcortical vascular dementia. Neurology 85, 1687–1693.
Zhao, L., Arbel-Ornath, M., Wang, X., Betensky, R.A., Greenberg, S.M., Frosch, M.P., Bacskai, B.J., 2015. Matrix metalloproteinase 9-mediated intracerebral hemorrhage induced by cerebral amyloid angiopathy. Neurobiol. Aging 36, 2963–2971.